VOLUME 23, 1961/62, No. 12 pp. 365-404 Published 16th October 1962

Philips Technical Review

DEALING WITH TECHNICAL PROBLEMS
RELATING TO THE PRODUCTS, PROCESSES AND INVESTIGATIONS OF
THE PHILIPS INDUSTRIES

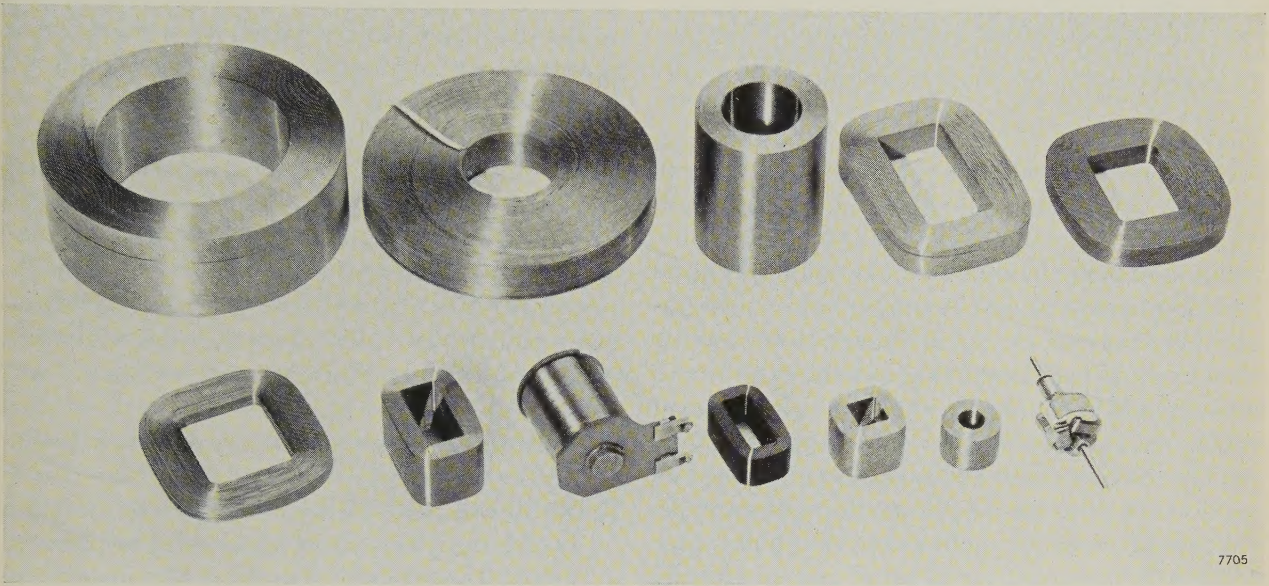

THE ORTHOCYCLIC METHOD OF COIL WINDING

by W. L. L. LENDERS *).

621.3.045.16

Orthocyclic winding is a method developed by Philips for obtaining coils whose turns are stacked in the most compact fashion possible. Such coils have certain particularly good properties including good heat conduction, even distribution of electric field strengths, and the highest possible space factor (which means that the coil dimensions, and hence also the statistical spread therein, are reduced to a minimum).

Any device exploiting electromagnetism contains one or more coils or windings made of insulated copper wire. The performance of the device and certain of its more important characteristics, such as size, weight and price, are to some extent dependent on the success with which the basic ingredients of coil design have been mixed. We are referring to the number of turns, the gauge of the wire, the shape and volume of the coil and the method employed for winding it. This hetrogeneous collection of variables opens the door to a great variety of coil properties. The range of possibilities becomes even greater where, as is usually the case, the magnetic flux produced by the coil passes through a ferromagnetic material, since the magnetic properties of these materials differ considerably and there is further a wide choice in the dimensioning of the magnetic circuit.

One aim that is generally striven for in the coil design is to get the highest possible *space factor*. In this context the space factor F means the ratio between the aggregate cross-sectional area of the turns inclusive of insulation and the area of the rectangle enclosing them ($ABCD$ in *fig. 1*). F is dependent on the shape of the wire (though we shall only concern ourselves here with *round* wire) and on the way in which it is wound. Inevitably there are interstices between the turns, and these represent wasted space, so that F is less than unity even

---

*) Radio, Television and Record-playing Apparatus Division, Philips, Eindhoven.

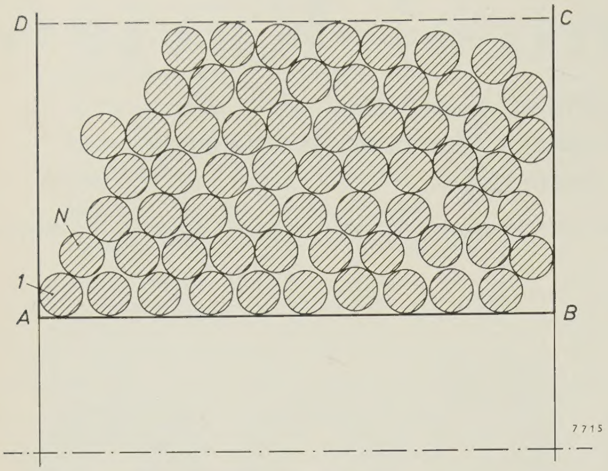

Fig. 1. Cross-section of irregularly wound coil.

in an ideal coil, though it may be only very little less. In a non-ideal coil, in other words in an irregularly wound one (fig. 1), F is considerably smaller than unity. The theoretical maximum space factor can actually be attained with a winding method which has been worked out at Philips and which we call the *orthocyclic* method. The method and its applications form the subject of the present article.

But first of all the importance of a high space factor will be demonstrated: let us take as example a telephone relay or selector embodying a coil which has not been wound by the orthocyclic method, and which provides a required number of ampere-turns at a certain rated voltage. Now let us suppose it proves possible, by adopting a better winding method to accommodate (say) 1.7 times as many turns of the same wire in the same space; the adoption of orthocyclic in place of "wild" winding does in fact result in an improvement of this order. The resistance of the new coil is 1.7 times that of the old; at the same voltage, the current is $1/1.7 \approx 0.6$ times what it was before. The number of ampere-turns remains the same, so that this design requirement continues to be satisfied; but the power consumption of the new coil is only 0.6 times that of the old one. In a telephone exchange, where the number of relays and selectors is large, the resulting economies are appreciable: less power-supply capacity is required, lighter-gauge wiring and cables can be used, and less energy is dissipated as heat.

Coils wound "wild" and coils with interleaved insulation

We shall first discuss two common ways of winding coils. *Fig. 2* shows a coil with the first layer completed: the turns cross the axis of the coil at an angle $90° - \alpha$. They have been wound from left to right, and form a left-handed helix. The second layer will run from right to left; it cannot be wound with the same neatness as the first. It ought to form a right-handed helix. In practice, however, its regularity will continually be disturbed because the wire has a tendency to lie in the grooves between the turns of the first layer, but since the two helices do not interlock, the wire of the second layer can only follow the grooves for short distances. Hence the irregularities will become ever greater as the winding of the coil proceeds, to such a point that it is soon no longer possible to distinguish one layer from the other. It is for that reason that we call this "wild winding".

The advantages of this primitive coil-winding method are that it is quick, that it can be done on a very simple machine, and that little time need be spent on the training of the operator. But examination of fig. 1, which represents a section through a coil wound by the "wild" method, will soon make it plain that this procedure has the following drawbacks:

1) The coil has a much smaller space factor than a neatly wound coil.
2) There will be a considerable random variation in the space factors of such coils. In order to reduce the number of rejects, the design will have to be based on almost the lowest space factor likely to be obtained. The variation in the space factor is associated with a variation in the average length of wire constituting a turn, and hence in the resistance of a coil.
3) Once the winding process starts to "run wild", some turns, particularly those at the sides, will inevitably end up nearer the axis than they

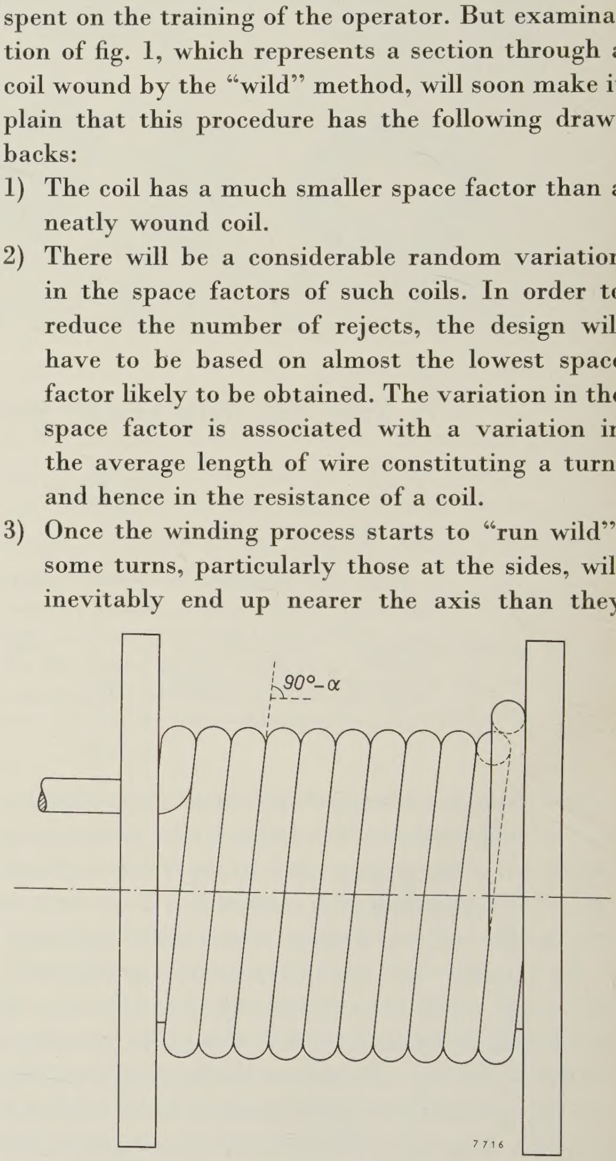

Fig. 2. Single-layer coil wound from left to right and having the form of a left-handed helix. The turns cross the axis of the coil at an angle of $90° - \alpha$. Irregularities will develop when the second layer is wound from right to left, and it will not be long before the winding process "runs wild".

ought to be, so that there will be relatively high voltages between turns lying in close proximity.

In consequence of (3) there is no way of knowing U_n, the highest voltage arising between contiguous turns of an irregularly wound coil with a voltage U across its ends; nor, therefore, is there any way of assessing the risk of breakdown in a coil carrying AC and of corrosion in a coil carrying DC. If the coil were regularly wound, all this would be known: for a winding consisting of l layers,

$$U_n = 2\,U/l. \quad . \quad . \quad . \quad . \quad . \quad . \quad . \quad (1)$$

(U_n is the voltage between the first turn of one layer and the last turn of the next.) Fig. 1 illustrates the worst case that can arise, that being when the last turn (N) lies on top of the first one (*1*).

To overcome these difficulties, it is a common practice to lay a strip of paper or other insulating material on each layer as it is completed; sometimes the insulation is inserted every two layers. This can be done automatically, so no loss of time is entailed. The great advantage of using interleaved insulation is that even and uniform layers are obtained: the paper prevents the layer which is being wound from being disturbed by the pattern of the layer underneath. The effect is as if a new start is made with each layer. Eq. (1) holds in this case and, moreover, the interleaved paper improves the breakdown voltage. Yet the space factor remains small: the gain obtained by regularity is cancelled out because the paper takes up some space, and because spaces also have to be left on either side of the coil (*fig. 3*). If the layers were wound over the whole breadth of the paper, the end turns would be liable to slip off.

Orthocyclic coils

We have seen that in "wild" coil winding it is impossible for regularity to be maintained after the first layer. The reason is that the tendency of the wire to lie in grooves formed by the preceding layer conflicts with the need for adjacent layers to have opposite helical configurations. The condition relating to orientation can be expressed in another way: if the turns of the first layer lie at an angle of 90° — α to the coil axis (fig. 2), then those of the second layer should lie at an angle of 90° + α. It follows that the difficulty disappears if α can be reduced to zero, in other words, if the first layer can be wound in such a way that each turn, or at least the greater part of each turn, crosses the axis *orthogonally*.

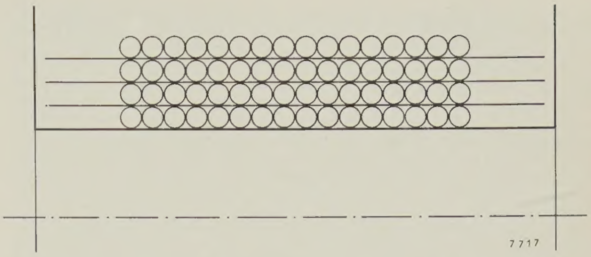

Fig. 3. Cross-section of coil with interleaved insulation. The turns are arranged in an orderly manner but the space factor is still small because the insulation takes up some space, and because some space has to be left free on either side of the layers.

Fig. 4 shows the pattern the first layer would have to assume in this case. Now, with a little care

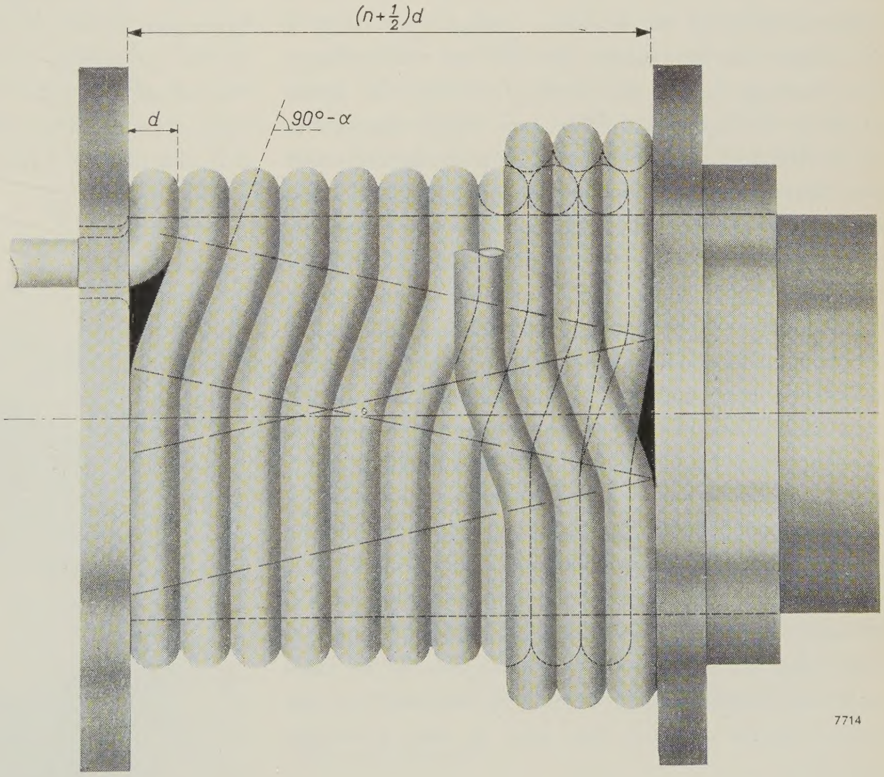

Fig. 4. A round orthocyclic coil at the stage where the first layer and a few turns of the second layer have been wound. Over about 90% of its length, each turn crosses the axis orthogonally. The remaining, inclined portion is known as the crossover; together the crossovers of one layer form a crossover line. Except for their crossover portions, the turns of the second layer lie neatly in the grooves formed by those of the first layer.

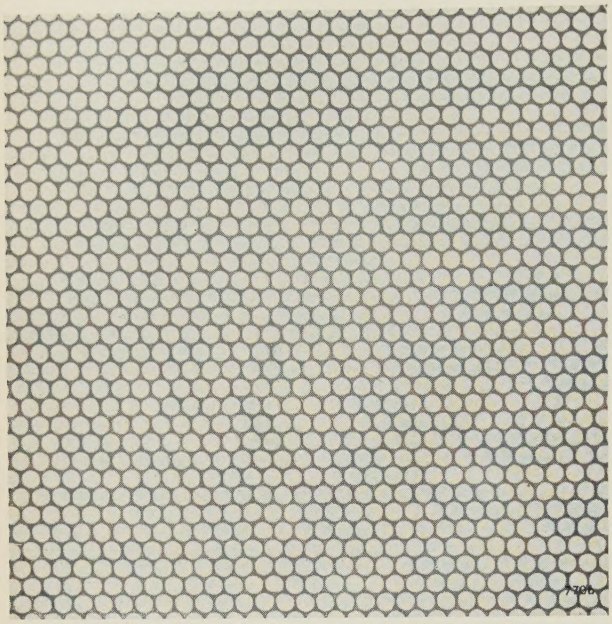

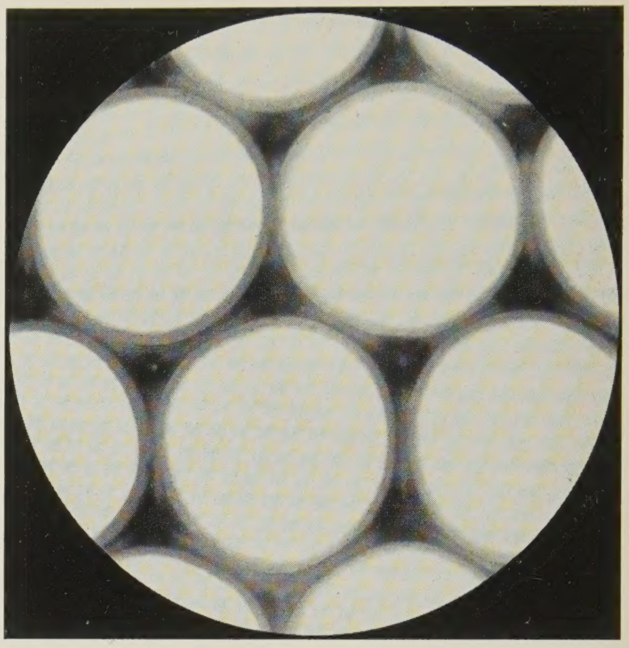

Fig. 5. Section revealed by sawing through an orthocyclic coil wound with copper wire of diameter 50 μm; the photograph on the left is 48 times, that on the right 600 times actual size. In virtue of the perfect orderliness and extreme compactness of the stacking pattern, the highest possible space factor has been achieved.

and ingenuity it is in fact possible to wind the first layer in this fashion, and it has been found that thereafter no difficulty is encountered in stacking succeeding layers evenly; this optimum stacking is the characteristic feature of what we call *orthocyclic winding*, by reason of the fact that the turns must lie orthogonal to the axis. The remarkable regularity and compactness of orthocyclic coils will be evident from the photographs (*fig. 5*) of a section revealed by sawing through a coil of this kind.

Crossovers

Obviously, the orthogonality requirement cannot be satisfied over the whole length of the turn. We use the term *crossover* to denote that section of each turn which lies out of the orthogonal (see fig. 4). Together, the crossovers of one layer form a *crossover line.*

In coils with a circular cross-section the crossover occupies about 10% of the total turn length. The crossover lines run through the coil in a zigzag fashion and their ends, as seen in the cheek of a finished coil, form an Archimedes' spiral (*fig. 6*). In coils with rectangular cross-section, crossovers in the lowest layers occupy one side of the rectangle (*fig. 7*).

Coil thickness and space factor

The thickness of orthocyclic coils is slightly greater in places where crossovers have been made. Let us first consider the places where no crossovers are present. Here it is only the first layer that contributes the full diameter of the wire d to the thickness of the coil. Because they lie in the grooves of the preceding layer, all layers other than the innermost contribute only $\frac{1}{2}\sqrt{3}d$ (*fig. 8*). Accordingly, the crossover-free portion of an orthocyclic coil comprising l layers has a depth of

$$[1+\tfrac{1}{2}\sqrt{3}(l-1)]d\,,$$

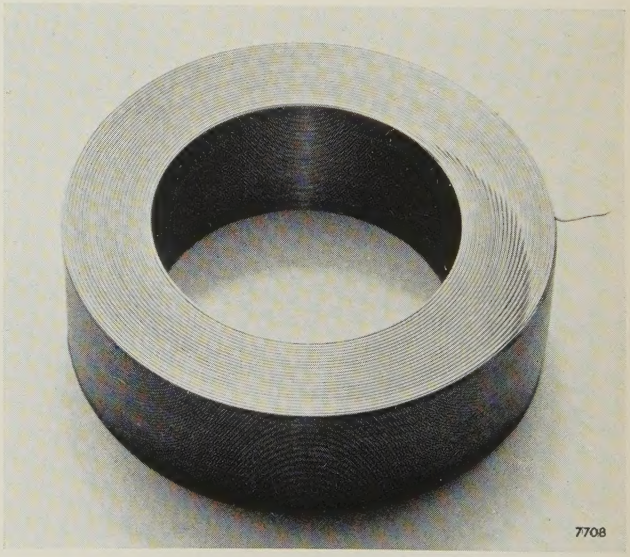

Fig. 6. Round orthocyclic coil. The ends of the crossover lines form an Archimedes' spiral in the cheek of the coil.

which, for a large number of layers, is roughly $\frac{1}{2}\sqrt{3}ld = 0.87ld$.

In considering the portion in which crossovers are present, round and rectangular coils must be dealt with separately. In *round* coils, the number of successive layers whose crossovers overlap does not exceed three; the local increase in coil thickness due to crossovers does not therefore exceed $3(1-\frac{1}{2}\sqrt{3})d = 0.4d$. Whether this is important or not depends entirely on circumstances. In *rectangular* coils the length of the crossovers, those of the lower layers at least, is the same at that of the side on which they lie (fig. 7*b*). Here, then, the crossovers are stacked one above the other, and the increase in thickness they occasion will be greater than the corresponding increase in a round coil with the same number of layers.

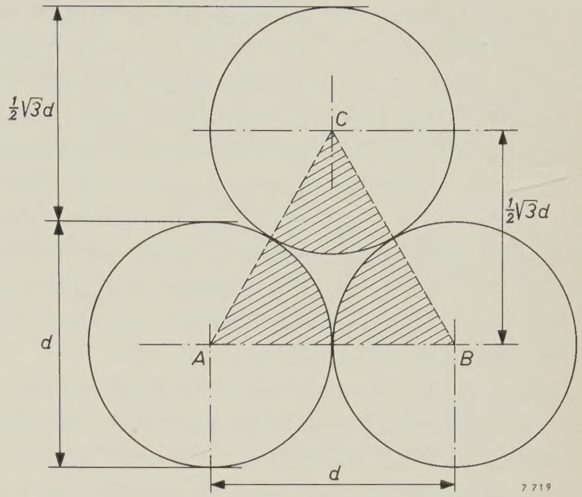

Fig. 8. Section through three contiguous turns in an orthocyclic coil wound with wire having an outside diameter *d*. If the crossovers and the "edge effect" be neglected, the space factor is the proportion of triangle *ABC* occupied by the hatched areas, i.e. 91%.

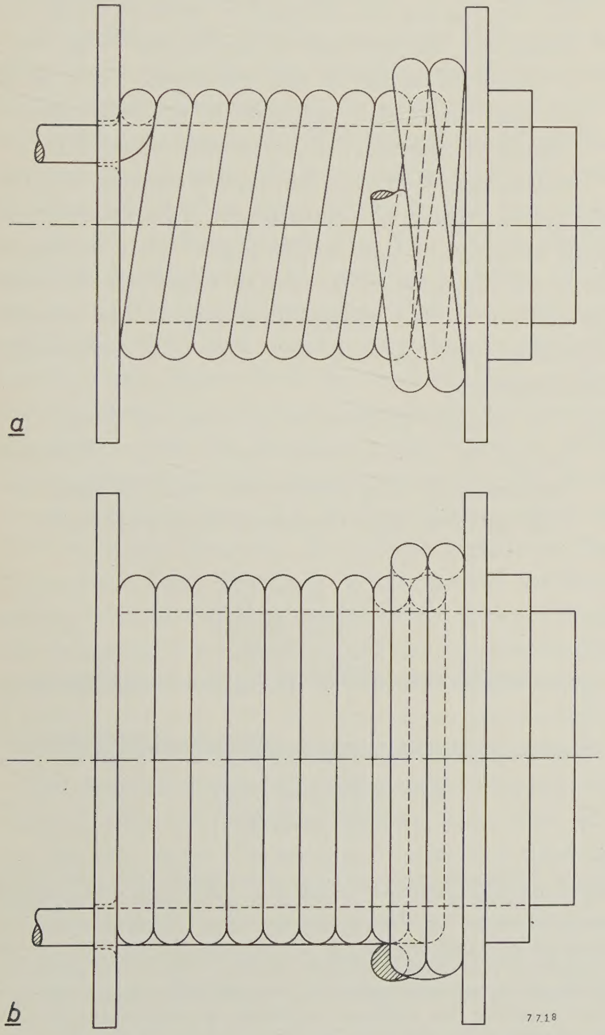

Fig. 7. Two faces of a rectangular orthocyclic coil, (*a*) that on which the crossovers are made, and (*b*) one of three faces on which the turns lie orthogonally.

We shall take the symbol F_0 to denote the "pure" space factor of an orthocyclic coil, in which no account is taken of the crossovers and of a second effect that will be dealt with below. F_0 is easily calculated: it is the ratio of the total area of the three hatched sectors in fig. 8 to the area of the equilateral triangle *ABC*:

$$\frac{\frac{3}{6}\times\frac{1}{4}\pi d^2}{\frac{1}{4}\sqrt{3}\,d^2}=\frac{\pi}{2\sqrt{3}}=0.91.$$

But so far we have ignored the fact that certain turns of the coil are not completely surrounded by other turns; the grooves in the innermost and outermost layers and in the cheeks of the coil are not utilized. The magnitude of this "edge effect" — to which, of course, non-orthocyclic coils are also subject — depends on the shape of the coil's cross-section. It may be important in the case of long, thin coils (in which the number of turns per layer is large relative to the number of layers) and still more so for flat, disc-shaped coils (in which the number of layers is large relative to the number of turns per layer). Still, even in the latter case, the true space factor F is unlikely to fall short of F_0 by more than one or two percent.

Because the space factor remains much the same from one coil to another, orthocyclic coils exhibit a particularly small random variation in external dimensions. The size of the coils is determined entirely by the outer diameter of the wire, the number of turns per layer and the number of layers.

The coil mandrel

Generally coils are wound on a former or bobbin made of impregnated paper or plastic; the bobbin affords mechanical protection and additional electrical insulation. Such bobbins are not as a rule up to the standard of dimensional exactitude required for orthocyclic winding. That greater precision is called for by this coil-winding method will be clear from the fact that each layer must consist of exactly the same number of turns n; the distance between the cheeks of the coil former must therefore be $(n+\frac{1}{2})d$, and experience has shown that deviations from this dimension must not exceed $\pm 0.2d$. This requirement is a severe one, particularly where it is a matter of winding very thin wire (with a diameter of 50 μm, for example).

Orthocyclic coils are not wound on a bobbin, then, but on a rigid metal mandrel that has been carefully machined to close tolerances. It is only after removal from the mandrel that the completed coil is mounted on a bobbin and provided with additional insulation.

The wire

In fig. 4 it has been tacitly assumed that in orthocyclic winding no clearance is left between turns of the same layer. This tight packing means that d must remain within particularly close limits. For example, if at a certain point in the wire its outside diameter should increase by 1%, only 50 turns later it would be riding on top of a turn in the preceding layer, instead of lying in the groove; the next turn would slip off the turn beneath, leaving a gap of $\frac{1}{2}d$. Thus disturbed, the regularity of the coil would be irremediably lost, and the disorder would worsen progressively.

The above tolerance of $\pm 0.2d$ for the layer breadth imposes a tolerance of $\pm 0.2d/n$ for the outside wire diameter. If for example d is nominally 100 μm and there are $n = 120$ turns per layer, then $0.2d/n = 0.17$ μm. In wire manufacture, the bare copper is reduced to the desired gauge by drawing through a die. Consequently the spread in the diameter of bare copper wire on a given reel is negligibly small ¹). An "enamel" covering is the only kind of insulation suitable for wire that is to be used for orthocyclic coil winding. The deposition of the "enamel" (which is really a type of varnish) is an easily disrupted process which must take place under strictly defined electrical, chemical and mechanical conditions ²). It may be regarded as something of an achievement that ways and means have been found of keeping the spread in d to within ±1% for a given reel of enamelled wire. Yet this is still six times more than the tolerance required in the above example.

There are two expedients whereby enamelled wire with an excessive spread in d can nevertheless be utilized for orthocyclic winding: a clearance can be left between turns, or the wire can be redrawn.

1) The variation in d can be allowed for by winding the first layer with a small clearance between the turns. It has been found in practice that the clearance must not exceed $0.03d$, otherwise the turns of the second layer will push those of the first layer too far apart. As can be imagined, the maintenance of an inter-turn clearance of a few microns calls for a rather complicated winding machine which accurately controls the pitch of the winding. We shall return to this problem later.
2) Wire exhibiting an excessive spread in d can be rendered suitable for orthocyclic winding *without* inter-turn clearances by redrawing it, i.e. by passing the enamelled wire through another die. The aperture of the die used must have a diameter equal to the minimum value of d, so that all thicker portions of the wire are reduced to this particular outside diameter.

Redrawing involves a perhaps somewhat surprising phenomenon: the variations in d are transferred, with a change of sign, to the copper core; in places, then, the diameter of the core is reduced in the same proportion as the outside diameter of the enamel covering (*fig. 9*), and this has two undesirable consequences:

a) The copper hardens on account of plastic deformation and so loses some of its pliability; consequently the crossovers tend to lengthen, and it is less easy to control their positioning.

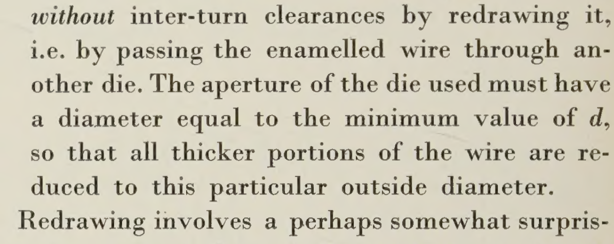

Fig. 9. Schematic representation of enameled wire undergoing the redrawing process. The aim is to get insulated wire whose outer diameter is everywhere the same. Besides producing the desired effect, redrawing transfers to the copper core the variations that were originally present in the outer diameter. *1* represents the wire still to be redrawn, which has a constant core diameter but exhibits variations in outer diameter, *2* is the drawing die, and *3* is the redrawn wire, which has a constant outer diameter but exhibits variations in core diameter. The thickness of the insulation and the variations therein have been exaggerated for the sake of clarity.

---

¹) Slightly bigger differences of diameter can naturally be expected in wire from different reels, which has been drawn through different dies.

²) R. J. H. Alink, H. J. Pel and B. W. Speekman, Manufacture and testing of enamelled wire, Philips tech. Rev. **23**, 342-351, 1961/62 (No. 11).

b) Since the diameter of the copper has been reduced in all the places where d was in excess, the electrical resistance per metre will have increased; if d was on average $a\%$ too large, the resistance increase will be about $2a\%$.

Attention is being devoted, in wire manufacture, to making the spread in d even smaller than it is at present, so that redrawing will involve less deformation, the above-mentioned disadvantages of the treatment thus being minimized.

In consequence of the variation in the core diameter of redrawn enamelled wire, orthocyclic coils wound from such wire exhibit a certain variation in resistance values. This, however, is generally smaller than the variation in the resistance of coils wound by the "wild" method. In the latter case the lack of uniformity in coil resistance is due, as stated above, to the considerable spread in the space factor and hence in the total length of wire that goes into the coil.

Orthogonal wire feed arrangements in coil winding

As we have seen, the characteristic feature of an orthocyclic coil is that the greater part of each turn lies in a plane at right angles to the axis. Accordingly, feed arrangements for the winding machine must be such that the wire coming off the reel likewise remains at right angles to the coil axis, at any rate within close limits. This aim might be achieved by dispensing the wire via a sheave wheel set up at a sufficient distance from the machine; in practice, the wheel would have to be a good many metres away. Apart from the inconvenience of the set-up, vibration in the long stretch of wire between the sheave and the machine could interfere with the regularity of the winding process. For that reason we make use of a guiding sheave which is free to move laterally, and which maintains the orthogonal feed direction automatically without having to be set up at a considerable distance from the machine. The device is shown schematically in *fig. 10*.

"*Thermoplac*" *wire*

The finished orthocyclic coil would fall apart on removal from the winding mandrel if it were not for the fact that "Thermoplac" wire [3]) is used in orthocyclic winding. The insulation of this wire has a thin thermoplastic coating. Before the coil is taken off the mandrel, it is warmed in order to fuse and bond the coatings on contiguous turns. Cooling results in a sturdy self-supporting coil. The thermoplastic film need only be about 2 μm thick. It can withstand the drawing process.

All the following methods are suitable and are in fact employed for heating the coil while still on the mandrel.

a) Baking in an oven.

b) Induction heating in an HF magnetic field (most of the heat is generated in the mandrel and passes to the coil by conduction).

c) Heating the coil by passing through it a current from an external source.

d) Short-circuiting the coil and inducing in it an alternating current (normally of mains frequency).

In methods (c) and (d), as against (b), heat is developed in the coil itself and the mandrel acts as a sink. It is therefore necessary, if either of these

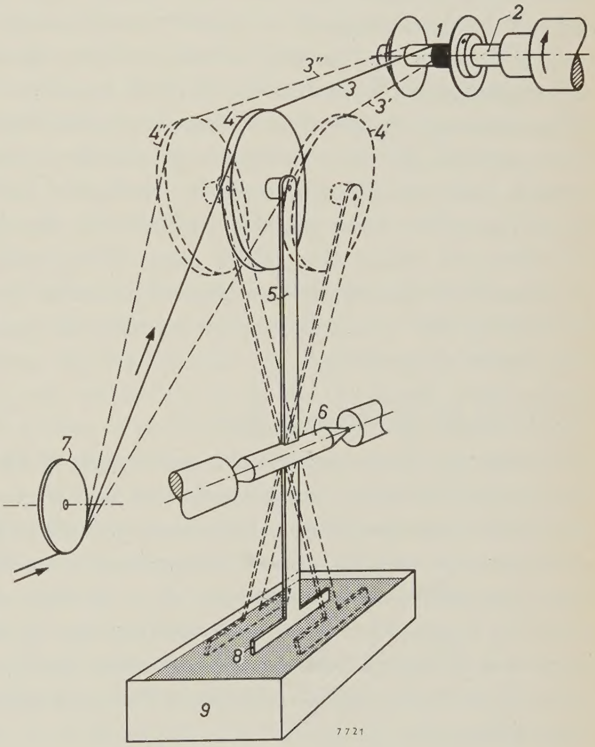

Fig. 10. Automatic arrangement to ensure that wire coming off a reel (not shown) will at all times be orthogonal to the coil axis, irrespective of the position of the turn being wound. The coil *1* is being wound on a mandrel turning about axis *2* and fed with wire *3* via a sheave wheel *4* on an arm *5* pivoting on a pin *6* that is orthogonal to *2*. Wire from the reel goes to *4* via a fixed sheave *7*. The point at which it leaves *7* is in line with *6*. By reason of the tension in the wire, sheave *4* automatically takes up position *4'* when a new layer is started, and moves to position *4''* as the layer is completed. If the small deviation due to the finite length of arm *5* be discounted, the wire dispensed to the mandrel remains orthogonal to axis *2* as it repeatedly passes from position *3'* via position *3* to position *3''*.

An extension to arm *5* carries a vane *8* which is immersed in an oil bath *9*. The oil provides enough damping to prevent transverse oscillations of the arm.

---

[3]) See the article cited in footnote [2]), p. 347.

two methods is used, to ensure adequate heating of those parts of the coil which are in contact with the mandrel while guarding against overheating of the remainder. In practice this means that the desired temperature must be attained within a few seconds. This is quite feasible with method (c) provided the resistance of the coil is low enough; fast heating of a coil having a high resistance would require a voltage involving the risk of breakdown between the first and last turns via the metal mandrel. Method (d) does not endanger the insulation of the coil because the terminals are shorted. It does, however, necessitate a core carrying a primary winding marrying with the type of coil being manufactured, and the cost of this will only be acceptable if the coils are to be turned out in sufficient quantity.

A closer look at certain aspects of orthocyclic winding

The exact manner in which orthocyclic winding can best be done depends on various circumstances, among these being the shape of the coil (round or rectangular) and the batch size (a small number of coils or enough to justify continuous production). Here we shall divide orthocyclic coil-winding procedures into two classes, those in which the first layer is wound and the pattern established by hand, and those in which this initial phase is done by machine. The two classes correspond more or less to the two cases of production on a small and on a large scale respectively.

Patterning the first layer by hand

If done by hand, orthocyclic patterning of the first layer calls for a certain amount of skill on the part of the operator. This is not a serious drawback so long as the number of coils to be made is small. However, only redrawn wire can be used, since it would be impossible, by hand, to maintain the small inter-turn clearance that is necessary when winding with wire whose outside diameter has not been corrected.

In these circumstances a simple winding machine will suffice, consisting of a spindle running easily in good bearings, a source of mechanical power and a revolution counter. The mandrel must have one fixed and one movable flange, the position of which can be accurately adjusted; the whole must have been carefully machined. Orthogonal wire feed arrangements are necessary (fig. 10). Redrawing of the wire can be combined with the winding operation.

Once the first layer has been wound and the movable flange correctly set, winding can be continued mechanically; it has been found in practice that the subsequent turns automatically adopt the correct "lie", the same regular pattern repeating itself from layer to layer. But care must be taken to see that the regularity of the winding process is not disturbed by incidental troubles such as vibration in the wire coming off the reel and — when very thin wire is being wound — the intrusion of dust particles. Insofar as it is not limited by such interfering effects, the winding speed can be stepped up to about 10 000 turns per minute from the second layer onward.

Forming the pattern mechanically

Mass-production requirements have led to the mechanization of the process whereby the orthocyclic pattern is established in the first and repeated in subsequent layers of the coil. The resulting winding machine is considerably more complicated, as will be clear from the account that now follows.

The separation of the mandrel flanges is so adjusted that there is just enough room for the prescribed number of turns per layer when the wire has its maximum diameter. By leaving a small clearance between turns it is possible to achieve even distribution, over the same breadth, of wire which has not been redrawn and whose diameter is (say) 3% below the maximum value. Even spacing of the turns is effected automatically by a shuttle arrangement that moves intermittently along a line parallel to the axis of the coil.

During the winding of the first layer, the shuttle is motionless for part of each revolution of the mandrel; it is during this interval that the orthogonal portion of the turn is produced. Oversimplifying for a moment, we can say that immediately a crossover is due to begin, the shuttle moves abruptly over a distance s equal to the wire diameter d plus the inter-turn clearance t.

This simplified description only holds good for a shuttle that is close to the mandrel — between its flanges, in fact. But if this was so in practice it would be impossible for the layer to extend from flange to flange, since the breadth of the greave must necessarily be greater than the diameter of the wire it guides on to the mandrel. Accordingly, the distance between the shuttle and the mandrel axis must be at least half the mandrel flange diameter. But if it is placed further away from the mandrel, each time the shuttle advances it must temporarily overstep its cumulating displacement $s = d + t$ by an amount s_e; see *fig. 11*, which shows the crossovers on a rectangular coil. If the shuttle did not travel this extra distance it would pull the wire against the preceding turn, the inter-turn clearance would be locally reduced to zero (along a line running transversely over the layer), and this part of the layer would be "waisted", the desired regularity thus being lost. The result, in a round coil, would be that the crossover became longer with every successive winding; in a rectangular coil with all the crossovers on one side of the rectangle, the layers would be narrower along one edge than along the other three.

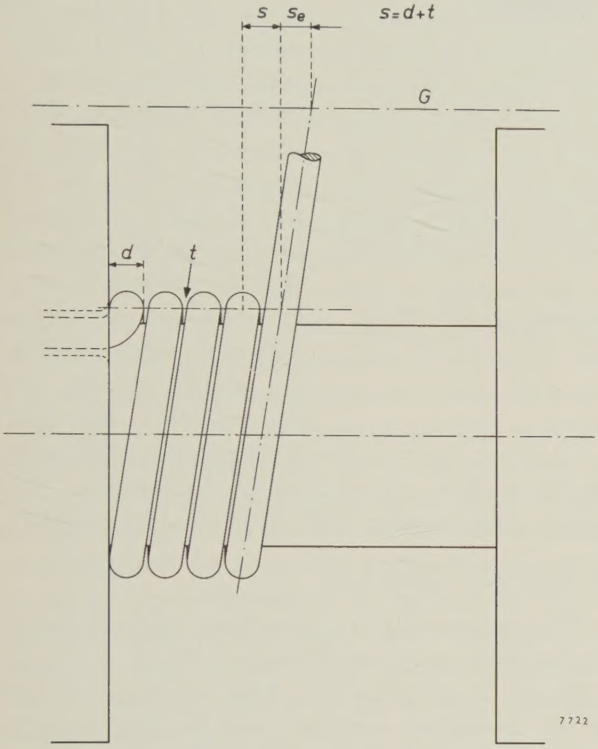

Fig. 11. Winding of the first layer of a coil with an inter-turn clearance *t*. Shuttle movement takes place along line *G*. Each time a crossover is begun, the shuttle, having undergone displacement through an interval $s = d + t$, must continue its forward movement, advancing over a further distance s_e, through which it will return as soon as the crossover is completed.

On completion of each crossover the shuttle must move back over the distance s_e.

There is no need for this extra shuttle displacement during the winding of the second and subsequent layers, the "lie" of their turns being determined by the grooves in the preceding layers.

While winding each turn of the innermost layer, then, the shuttle has to perform a somewhat complicated movement. The time available for its performance is the time taken by the mandrel to turn through the angle within which the crossover is made. This sets a limit to the winding speed. The crossover angle is 90° for square coils, and rather more or rather less for rectangular coils, depending on whether the crossovers are being made on the long or short side of the rectangle; for round coils the crossover angle is only 30° to 40°. It follows that the first layer of rectangular coils can be wound more quickly than the first layer of round ones.

Reasons why crossovers in rectangular coils must be confined to one side of the rectangle

Fig. 4 shows how the crossover lines run in zigzag fashion over the surface of a round coil. In rectangular coils the crossover lines have a tendency to do the same thing; but it is necessary to confine them to one side of the rectangle, as in fig. 7*a*, for otherwise the coil cannot remain orthocyclic. This is due to the fact that the length of the crossover, and hence also the inclination of the crossover line with respect to the coil axis, is dependent on the radius of curvature of that part of the turn which constitutes the crossover. If the crossover line should turn the corner, as it were, invading an adjoining face of the coil, it would do so at a point where the radius of curvature of the wire changes abruptly, and the angle of the crossover line with respect to the axis would also alter. The effect is as if the crossover line is bent by the corner of the rectangle, with the result that one turn is missed out. Starting at this point, the irregularity worsens progressively as further layers are added. Finally the winding process "runs wild".

There is a second reason why it is desirable to keep all crossovers on one face of a rectangular coil. Take for example the winding of a transformer with a core made up of E and I-shaped laminations: two sides of the rectangular winding, which we may call *A* and *C*, have to be accommodated inside the openings in the core, and the winding depth should therefore be as small as possible on these two sides. The endeavour will accordingly be to confine the crossovers to *B* or *D*, the sides of the rectangle lying outside the core.

A special winding mandrel, designed to provide effective control of crossover lines, enables all crossovers to be confined to one side of rectangular coils. The ends of the crossover lines form a pattern in the cheek of the coil, revealing whether the crossovers do in fact lie on one side of the rectangle, or whether they have invaded an adjoining side. They have done so in coil *a* in *fig. 12*, but not in coil *b*.

On sides *A* and *C* the winding — we still have a transformer coil in mind — will bulge slightly, to an extent dependent on the tension in the wire coming off the reel, and will therefore take up more space than necessary in the core openings. The bulge can be evened out by compressing the sides in question either during or after the heat treatment. There is no risk of damaging the insulation because

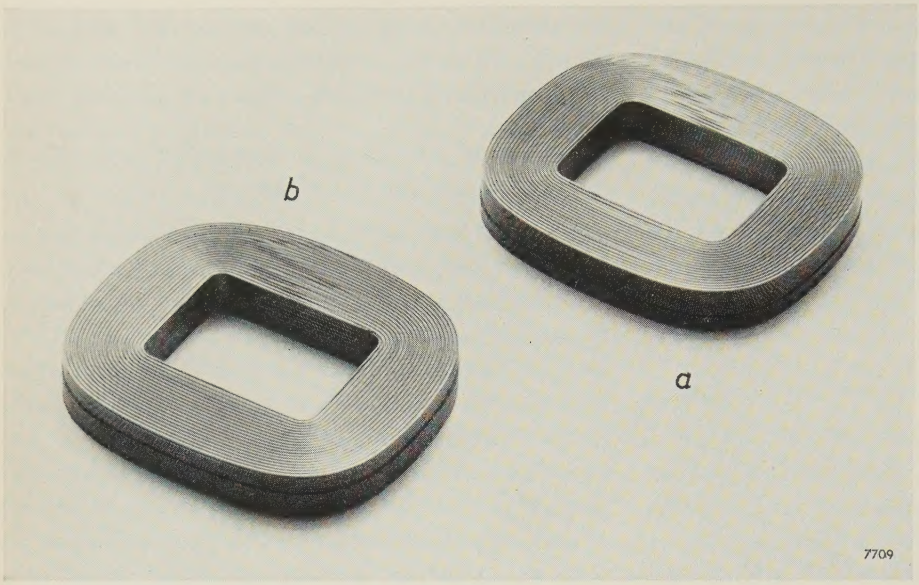

Fig. 12. Rectangular orthocyclic coils. The patterns traced in the cheeks of the coils by the ends of crossover lines reveal that in coil *a* the crossovers have "turned the corner", but in the case of coil *b* have been confined to one side.

sides *A* and *C* are free of crossovers. Coil *a* in *fig. 13* has not been compressed; coil *b* has been squared up on three sides.

Orthocyclic coils compared with types wound by other methods

The foregoing will have made it clear that orthocyclic coils possess two big advantages as compared with other kinds:

1) In orthocyclic coils the space factor attains the theoretical maximum value. In consequence, the random variation in the space factor, and hence in the overall dimensions of the coil, is extremely small.
2) Since each turn of an orthocyclic coil lies in its appointed place, the voltages between given pairs of turns are well defined; moreover, the greatest voltage between contiguous turns is as given by eq. (1). It is therefore possible to ascertain in advance whether U_n will be too high for the wire-covering and whether, accordingly, interleaved insulation will have to be used (in which case there will not of course be any point in winding the coil orthocyclically).

Further important properties which distinguish orthocyclic coils from other kinds will now be enumerated.

3) *Permanence of shape*

Thanks to the thermoplastic bonding agent the turns of an orthocyclic coil coalesce into a very sturdy unit, much stronger than a coil that has been wound "wild" out of wire having a thermoplastic coating of the same thickness. This greater robustness is due to the fact that the turns bind one another over their whole length, and it enables orthocyclic coils to withstand considerable mechanical stresses without loosening of the turns. In virtue of this property orthocyclic coils are particularly suitable for applications in which they are subject to severe vibration, as is the case with the rotor windings of electric motors and moving coils for loudspeakers. We shall revert to the subject of orthocyclic loudspeaker coils below, when dealing with individual applications.

4) *Good heat conduction*

The heat developed in a coil has to be dissipated via its outside surfaces. There is therefore a temperature gradient in the coil. With an eye to the life of the insulation, a ceiling must be fixed for temperatures arising in the coil [4]; but normally the point where the highest temperature prevails is

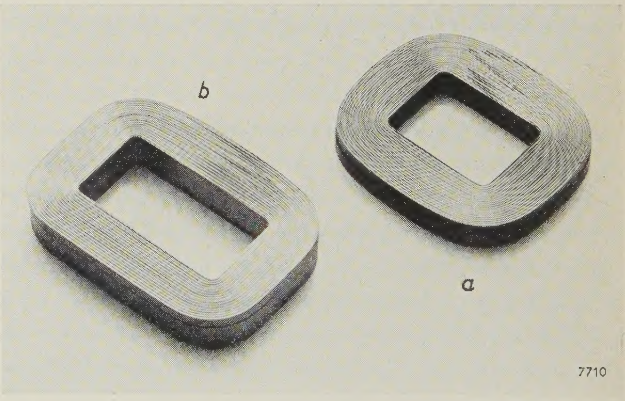

Fig. 13. Rectangular orthocyclic coils in which crossovers have been confined to one side of the rectangle. The faces of coil *a* bulge slightly. The three faces of coil *b* not containing crossovers have been pressed flat, with some saving of space as a result.

---

[4] In regard to the connection between life and temperature, see for example T. Hehenkamp, The life of ballasts for gas-discharge lamps, I. Transformers and chokes, Philips tech. Rev. **20**, 59-68, 1958/59.

inacessible for measurement, and in practice, by way of compromise, the average temperature is determined, this being worked out from the easily measured increase in electrical resistance resulting from the warming-up of the coil. The highest temperature arising in the interior of a non-orthocyclic coil may easily be 10 °C above the temperature of the outside surface and 5 °C above the average temperature.

Orthocyclic coils conduct heat so well that in normal use no perceptible difference of temperature arises between the interior and the outside. The thermal conductivity of orthocyclic coils, measured perpendicular to the wire, was found to be 1 W/m^2 per °C/m (or 0.85 kcal/mh°C), which is 20 times the value for coils with interleaved paper insulation. Hence, if a non-orthocyclic coil exhibiting the temperature differences just cited is replaced by an orthocyclic coil, the insulation of the latter will not be endangered if its temperature is allowed to rise 5 °C above the average temperature of the first coil. That higher temperatures are permissible in orthocyclic coils is fortunate in view of the fact that, on account of their better space factor, they occupy a smaller volume and are thus likely to have a smaller surface area than non-orthocyclic coils. By reason of better heat conduction an orthocyclic coil is warmer on the outside than a non-orthocyclic coil with the same internal temperature, and is thus able to dissipate heat at a given rate through a smaller surface area.

5) *High quality factor*

A direct consequence of the high space factor of orthocyclic coils is that less wire of a given gauge is needed to wind a coil with a given number of turns. On account of the smaller winding length the ratio of resistance R to inductance L is smaller than in non-orthocyclic coils; the quality factor $Q = \omega L/R$ is therefore relatively high.

6) *Small variation in inductance and self-capacitance*

In orthocyclic coils each turn has its exactly defined position, and in consequence of this the inductance and self-capacitance differ very little from the nominal values. This is of importance in connection with centre-tapped transformers, which, in telephony and other fields, have to satisfy high standards of electrical symmetry. If such transformers are wound by ordinary methods, exact balance can only be achieved by having recourse to trimming capacitors. These are generally superfluous if the transformer has been wound by the orthocyclic method.

Disc-shaped coils, consisting of narrow layers stacked to a considerable height, are called for in cases where very low self-capacitance is essential.

The random variation in the resistance of the coils has already been mentioned (page 371).

Applications of orthocyclic coils

Our factories have now been employing the orthocyclic winding method for several years. In the early days, of course, knowledge of certain factors affecting the product — tolerances for wire thickness and mandrel dimensions, the correct pattern for the first layer, and the like — was still incomplete. Because these matters had not yet been fully investigated, more had to be asked of the coil-winder in the way of skill and insight into the process than was required by the old, familiar method. For that reason a long training period was necessary, output was inclined to be small, and the rejection rate was sometimes high. As a consequence, at that time orthocyclic coils were comparatively expensive to make, and there could be no question of producing them in quantity. Initially, then, applications of the technique were limited to a few products in the professional class. At present all factors influencing the orthocyclic winding process are well under control, so much so that the method is being adopted in mass production.

A few examples of applications in both categories will now be given.

Professional applications

1) The 600 MeV CERN synchrocyclotron at Geneva is equipped with a modulator that causes the frequency of the accelerating voltage to sweep periodically (55 times per second) over a range extending from about 29 to 16.5 Mc/s. The frequency-modulating device is a gigantic "tuning fork" that acts as a vibrating capacitor [5]). The fork is excited by the field of a set of orthocyclic coils carrying current with a frequency of 27.5 c/s. The whole assembly is in a vacuum.

The main reasons for choosing orthocyclic coils were their high space factor (space was very limited), good heat dissipation and ability to stand up to vibration. During evacuation of the vacuum chamber it was found that the coils released very little gas, the pumping time thus being particularly short.

2) In incandescent lamp manufacture, the bulbs are filled with gas via an electromagnetic valve.

---

[5]) B. Bollée and F. Krienen, The CERN 600 MeV synchrocyclotron at Geneva, III. The tuning-fork modulator, Philips tech. Rev. **22**, 162-180, 1960/61 (No. 5). — The excitation system is shown in figs 11 and 12 of that article.

For constructional reasons it was highly desirable that the magnet dimensions be reduced to a minimum; an orthocyclic solenoid was therefore indicated.

3) For monitoring steam turbines, electronic equipment has been developed which keeps a continuous record of vibration amplitudes and the dimensional changes affecting various parts of the turbine [6][7]. For example, the eccentricity of the shaft is measured with the aid of a displacement pick-up working on the inductive principle, as illustrated in *fig. 14.* The pick-up windings form part of an AC bridge circuit. For zero eccentricity the bridge should be in balance; any deviation from dead true running should give rise to a signal proportional to the eccentricity of the shaft. It often happens in practice, however, that the temperatures and hence also the resistances of the different windings differ considerably. Consequently the bridge circuit is not always exactly in balance for zero eccentricity, and the signal it yields is not dependent on shaft eccentricity alone. The lower the resistance of coils having a given inductance value — the higher their Q factor, in other words — the smaller the error. In this respect, as we have seen, orthocyclic coils and windings have the edge over non-orthocyclic ones.

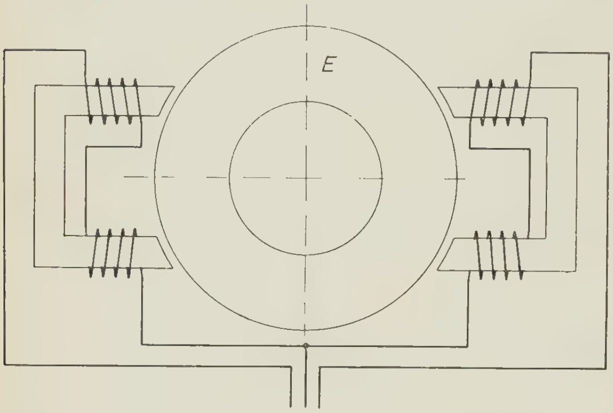

Fig. 14. Inductive pick-up for the continuous detection of eccentricity in a turbine shaft [6]. A disc E of nickel-iron alloy is mounted on the shaft. On either side of the disc is an iron yoke carrying windings that form part of an AC bridge circuit. Provided the two pairs of windings have the same resistance, the signal originating in the bridge will be proportional to the eccentricity of the shaft. A disparity in their resistances, due to temperature differences, gives rise to a measuring error. The higher the Q factor of the windings, the smaller this error is, and that is one of the reasons why the windings are made by the orthocyclic method.

The same considerations apply to other inductive types of displacement pick-ups used on turbines (see figs 9 and 10 of the above-mentioned article [6]).

4) Focusing coils for travelling-wave tubes. In this form of electron tube — one of the kinds used to generate or amplify centimetre waves — an electromagnetic wave propagates itself along a metal helix, through the centre of which passes an electron beam focused by a magnetic field [8]. The field must possess a certain distribution in the axial direction, and it must satisfy stringent requirements in regard to rotational symmetry. In most travelling-wave tubes the field is supplied by permanent magnets. However, in some high-power types a very strong field is required, extending over a considerable distance along the axis, so that an electromagnet is the only practicable means of focusing the beam. The desired distribution of field strength along the axis can be obtained by setting up three differently shaped coils side by side, two disc types being placed at either end of a long tubular coil. Besides offering the familiar advantages of small dimensions with a negligible statistical spread, round orthocyclic coils, by reason of their regular structure, satisfy the rotational symmetry requirement much better than do coils wound by the "wild" method.

Mention may be made here of one of the few cases in which orthocyclic winding was not a success. During design studies for a large X-ray apparatus in which the HT transformer was to be combined with the tube in a single block, it became evident that a smaller and lighter transformer would be desirable. Accordingly, the secondary winding with its interleaved paper insulation was replaced by an orthocyclic winding. However, this secondary had the drawback of excessive self-capacitance. It is true that this difficulty could be got over by substituting for the single secondary a set of flat orthocyclic disc windings connected in series, but the voltage between neighbouring windings was then so high (of the order of 10 kV) that corona and flashover gave rise to further difficulties. Adequate insulation between the disc sections would have meant spacing these so far apart as to cancel out completely the gain obtained by winding them orthocyclically.

Applications in mass production

Over recent years our coil winders have acquired such a degree of expertise in the orthocyclic tech-

---

[6] C. von Basel, H. J. Lindenhovius and G. W. van Santen, Electronic equipment for the continuous monitoring of turbines, Philips tech. Rev. **17**, 59-66, 1955/56.

[7] C. von Basel, Messanlage zur Überwachung von Dampfturbinen, Arch. techn. Messen V 8232-2, 221-224, October 1956.

[8] J. G. van Wijngaarden, A travelling-wave tube for the frequency band of 3800 to 5000 Mc/s, Le Vide **15**, 36-40, 1960.

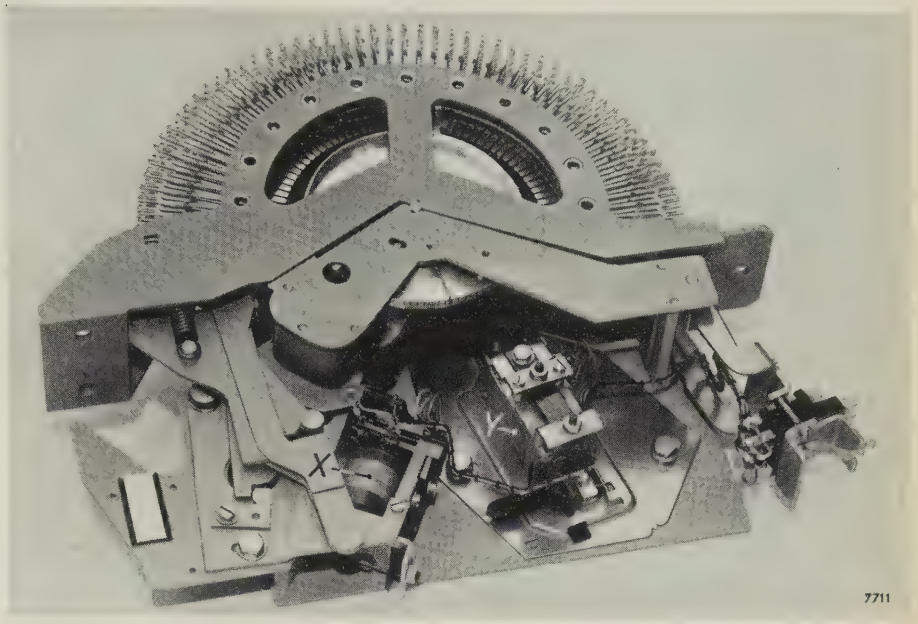

Fig. 15. Type U 45a high-speed uniselector [9]). Both coupling magnet X and stopping magnet Y embody orthocyclic windings.

nique that there is a growing tendency for it to be employed on a large scale in mass production. A few examples will now be given.

1) Selectors for telephone exchanges. The type U 45a high-speed uniselector (*fig. 15*), made by N.V. Philips' Telecommunicatie-Industrie, Hilversum [9]), embodies one electromagnet which couples the contact wipers to a continuously rotating shaft, and another which arrests them at the desired place. Both the coupling and the stopping magnets are energized by orthocyclic windings, which, as we saw at the beginning of this article, have the great advantage of saving power and so reducing the amount of heat developed, the numerous selectors and relays usually being the main source of unwanted heat in telephone exchanges.

2) Moving coils for loudspeakers are wound on a miniature bobbin that is subsequently glued to the cone. Thin-walled as the bobbin may be, it still takes up a certain amount of space in the air gap of the magnet, where even fractions of a millimetre count. Furthermore, the dimensioning of the gap has to allow for the deviations from exact circular shape which are exhibited by most bobbins in consequence of their lack of rigidity in the radial direction.

Thanks to a method which has been developed for attaching self-supporting coils to loudspeaker cones, and which provides a particularly strong bond between the two, an immediate advantage of winding the moving coils by the orthocyclic technique is that the bobbin can be done away with. If the coil consists of several layers, as it is bound to do if destined for a high-impedance speaker [10]), then orthocyclic winding will also reduce its thickness appreciably. In addition, the radial rigidity of orthocyclic coils is much greater than that of coils of older design. For various reasons, then, a narrower air gap suffices for an orthocyclic moving coil, and this pays off either in enhanced efficiency or in reduced magnet size. Another advantage is that orthocyclic coils are better able to stand up to vibration.

3) Self-supporting (but non-orthocyclic) moving coils have long been used in electrodynamic microphones. If the moving coil is wound orthocyclically the air gap can be narrowed, with a resulting increase in the sensitivity of the microphone.

4) In the winding of field coils for moving-iron voltmeters and ammeters, the change-over to the orthocyclic technique has allowed so many additional turns to be accommodated that the sensitivity of the meters is 2 to 2.5 times as great as before.

5) Being battery-fed, portable electronic products must be small in size and have the lowest possible power consumption. When an electric motor for battery gramophones and tape recorders was being designed, it was found that an orthocyclic rotor winding saved so much space that a much lighter rotor could be made if the "wild" method were abandoned in favour of the orthocyclic one. Also, because less iron was present, losses due to eddy currents were smaller, resulting in a good 25% saving in power consumption. A second advantage of orthocyclic rotor windings is the negligible variation in their weights, in virtue of which they are unlikely to be responsible for unbalanced distribution of rotor masses. *Fig. 16* shows the rotor with its three orthocyclic windings.

6) Ballasts for "TL" lamps in aircraft. By reason

---

[9]) J. M. Unk, A high-speed uniselector for automatic telephone exchanges, Philips tech. Rev. **18**, 349-357, 1956/57.

[10]) J. Rodrigues de Miranda, Audio amplifiers with single-ended push-pull output, Philips tech. Rev. **19**, 41-49, 1957/58.

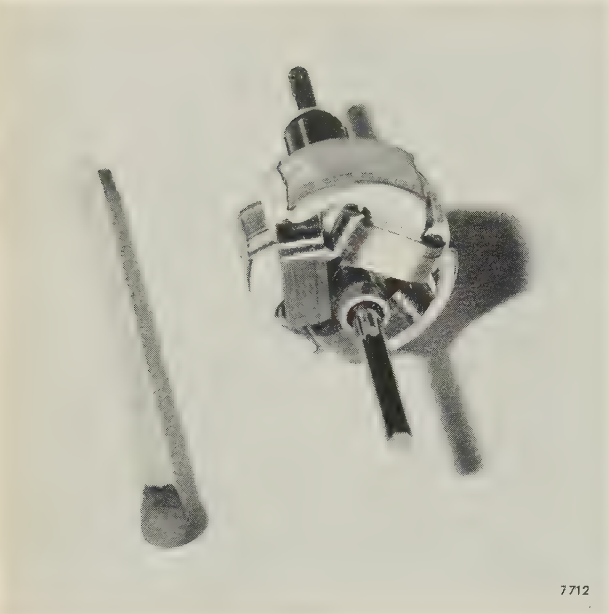

Fig. 16. Rotor of the electric motor incorporated in battery-operated portable gramophones and tape recorders. Employment of the orthocyclic technique for the three armature windings has allowed the size of the motor and its power consumption to be reduced.

of their high efficiency tubular fluorescent lamps are being employed more and more in the public transport sector [11]), including aviation. Passenger-carrying aircraft can now be equipped with (say) twenty 40 W "TL" lamps. In common with everything else that goes to equip aircraft, the weight of the ballasts must be cut to an absolute minimum. Employment of the orthocyclic technique for winding the choke coil has made it possible to bring down to 195 grams the weight of the ballast (consisting of a choke coil and a capacitor) for a 40 W lamp, rated for 115 V at 400 c/s, the standard aircraft electricity supply. The ballast in question may be seen in *fig. 17.*

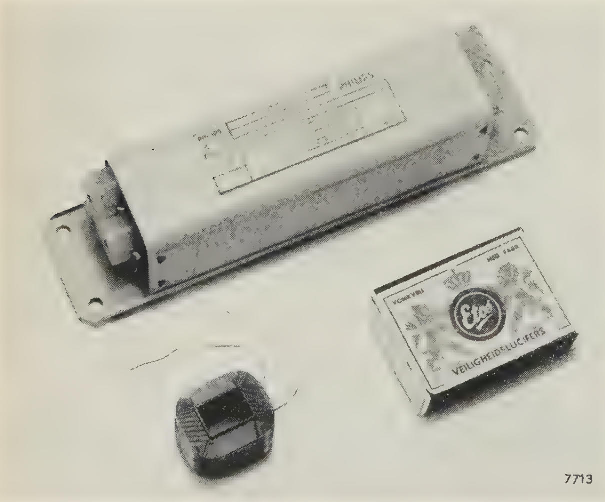

Fig. 17. Ballast for a 40 W "TL" lamp to work on the standard aircraft supply of 115 V at 400 c/s. Altogether, the choke coil and associated capacitor weigh only 195 g. Below, left, the orthocyclic choke coil.

7) Electromagnetically-controlled air valves. A

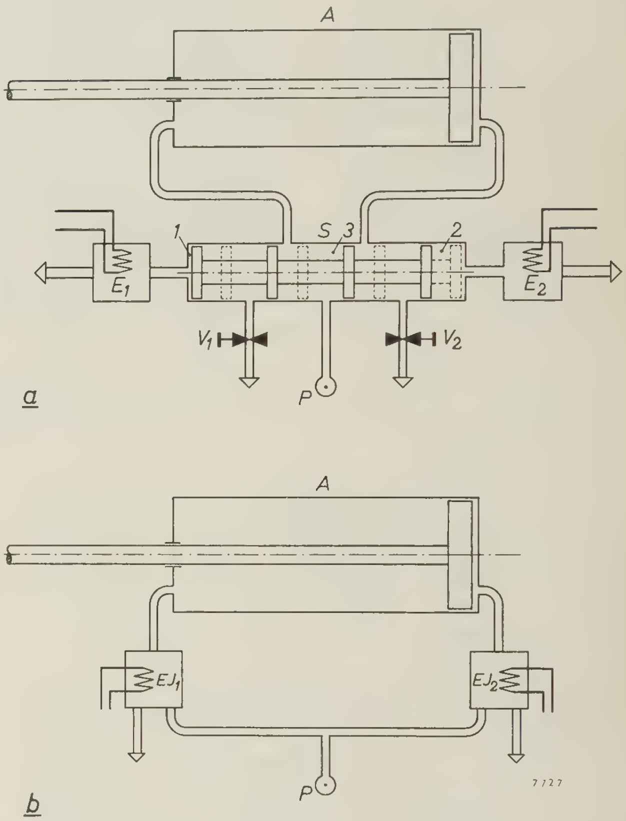

Fig. 18. *a*) Air cylinder A and associated pneumatic equipment. S piston valve, E_1-E_2 solenoid-operated air-control valves, V_1-V_2 adjustable bleed chokes. Compressed air enters the system from pipe P. When the pistons in valve S occupy the positions indicated by fully-drawn rectangles, the space in A to the left of the main piston is connected to P, and the air to the right of the main piston can escape via V_2. In these circumstances the cylinder piston is at the extreme right of its stroke. Spaces *1* and *2* in S are connected (by ducts not shown in the diagram) to space *3*, the pressure in which is at all times that of the compressed-air supply. So long as control valves E_1 and E_2 are closed, then, the air in *1* and *2* is at the same high pressure as that in *3*.

To shift the cylinder piston to the left, control valve E_2 is opened, whereupon air escapes from *2*, the valve pistons move into the positions indicated by the broken-line rectangles, compressed air from P is free to pass via *3* into the space on the right of the cylinder piston and the air in the left-hand side of A exhausts through V_1. The speed with which the cylinder piston travels to the left can be regulated by adjusting V_1. To return the cylinder piston to the right, E_2 is closed and E_1 is opened.

b) In the new system, control of air cylinder A is effected solely by means of EJ_1 and EJ_2, two "Electrojet" valves made by the Martonair Company. These supersede air control valves E_1 and E_2 as well as piston valve S, and accordingly their bore must be at least as great as that of S in (*a*). Having adjustable outlets, the "Electrojet" valves are further able to take over the function of bleed chokes V_1 and V_2. They embody orthocyclic coils, these having been chosen on account of their small size and good heat dissipation.

---

[11]) L. P. M. ten Dam and D. Kolkman, Lighting in trains and other transport vehicles with fluorescent lamps, Philips tech. Rev. **18**, 11-18, 1956/57.

favourite practice in machine building is to fit an air cylinder to supply mechanical power for certain movements which, as a rule, are initiated by switching an electric circuit. Until recently the air cylinder, essentially a simple device, had to be used in conjunction with a pneumatic circuit comprising, in addition to a filter and lubricating unit, a piston valve controlled by one or two solenoid-operated air control valves, one or two adjustable bleed chokes and the associated piping and fittings. An example of a circuit of this kind (many variations are possible) is given in *fig. 18a*.

These arrangements can be greatly simplified by using the "Electrojet" system designed and marketed by the Martonair Company of Amsterdam. Fig. 18*b* shows the "Electrojet" version of the circuit in fig. 18*a*: it will be noted that in addition to the air cylinder itself, only two electromagnetic valves of the new type are necessary, these having taken over the functions of the piston valve, the two air control valves and the two bleed chokes. The overall dimensions of the "Electrojet" valve are no greater than those of the air control valve in the original circuit. The new valve must however have a much bigger bore in order to do the work of the piston valve, and the electromagnet actuating it must therefore develop a stronger pull. One of the ways in which increased pull has been obtained is by using an orthocyclic solenoid which, thanks to good heat conduction, can be heavily loaded without overheating, and is thus able to supply the required higher number of ampere-turns.

The bore of the "Electrojet" valve is large enough for most of the air cylinders on machines used at Philips. It passes enough air at 5 atm to displace a 4″ diameter cylinder piston at a speed of about 17 cm/s against a force of 300 kg, or to enable a $1\frac{1}{4}''$ piston to travel at about 170 cm/s while overcoming a force of 30 kg.

The above examples will doubtless have sufficed to demonstrate the advantages of the orthocyclic winding method, and to illustrate the variety of its applications. It need hardly be added that the method can profitably be employed in many other cases.

Summary. The term "orthocyclic" is applied to a coil-winding method whereby the greater part of each turn is made to lie orthogonally with respect to the coil axis. Provided the correct pattern is established in the first layer and certain precautions are taken, subsequent layers will automatically fall into the same regular pattern, each turn fitting into its appointed place, a groove in the layer beneath. The turns are stacked in the most compact fashion possible, in consequence of which (1) the space factor attains its theoretical maximum value, (2) the highest voltage existing between contiguous turns is fully defined, and (3) the dimensions, inductance and self-capacitance of individual coils of the same type fall within very close limits. It is possible by winding with "Thermoplac" wire to obtain strong self-supporting coils which have invariable dimensions and stand up well to vibration. The thermal conductivity of orthocyclic coils is so high (1 W/m °C, or 20 times that of coils with interleaved paper insulation) that they display no appreciable temperature gradient, and their temperature can safely rise to a value higher than the average permissible in non-orthocyclic coils. In conclusion, various applications of orthocyclic coils (to focusing coils for travelling-wave tubes, electromagnet windings in uniselectors, field coils in moving-iron meters, rotor windings in small motors, etc.) are discussed and the resulting benefits enumerated.

FIZEAU FRINGES OBSERVED WITH AN INTERFERENCE MIRROR

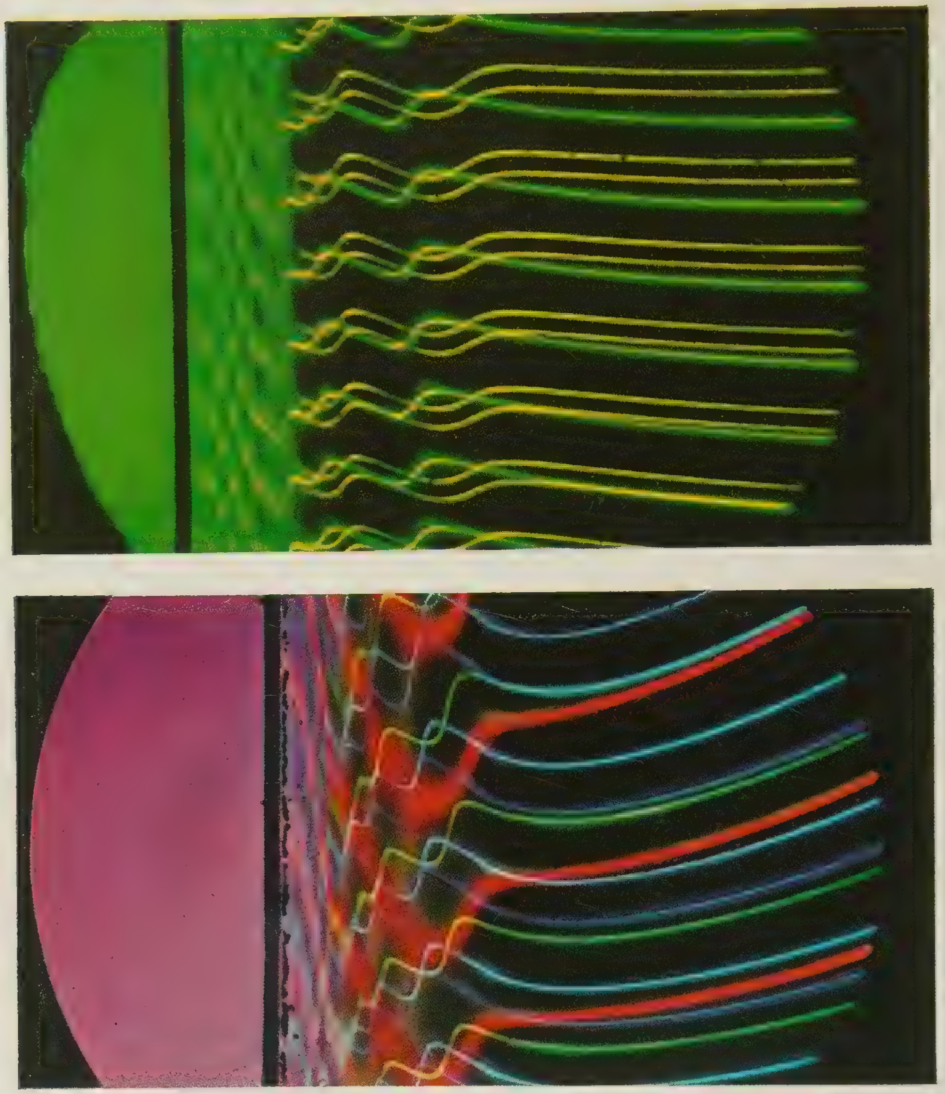

a

b

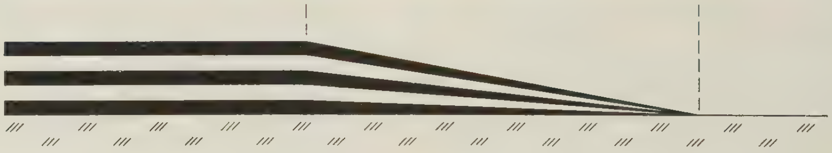

When a monochromatic beam of light is directed upon an interference mirror (consisting of thin dielectric layers of alternate high and low refractive index) which is placed a short distance from a half-silvered mirror, a pattern of relatively sharp interference fringes (Fizeau fringes) can be seen in transmission. These fringes represent lines of constant (optical) thickness of the space between the mirrors, and can therefore in general never intersect, even when several wavelengths are used.

The above photographs show the fringes for several different wavelengths at the same time (*a*: cadmium lines 4678-4800-5086-6438 Å; *b*: green mercury line 5461 Å, and yellow mercury doublet 5770-5791 Å) in the neighbourhood of the edge of an interference mirror, where the layers gradually taper to zero thickness (see drawing). It can be seen that here the fringes for different wavelengths intersect. This remarkable effect can be explained in terms of the wavelengths dependence of the phase with which a multilayer mirror reflects the light (phase dispersion). For further particulars see: G. Bouwhuis, A dispersion phenomenon observable on dielectric multilayer mirrors, Philips Res. Repts **17**, 130-132, 1962 (No. 2).

ERRATUM

The colour photographs on page 380 have been printed in a wrong position. The correct position is indicated below.

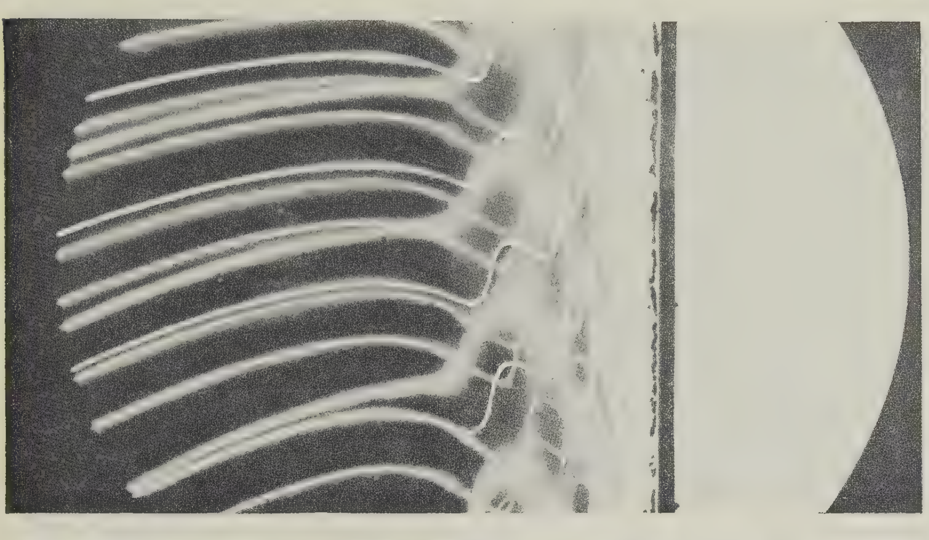

a

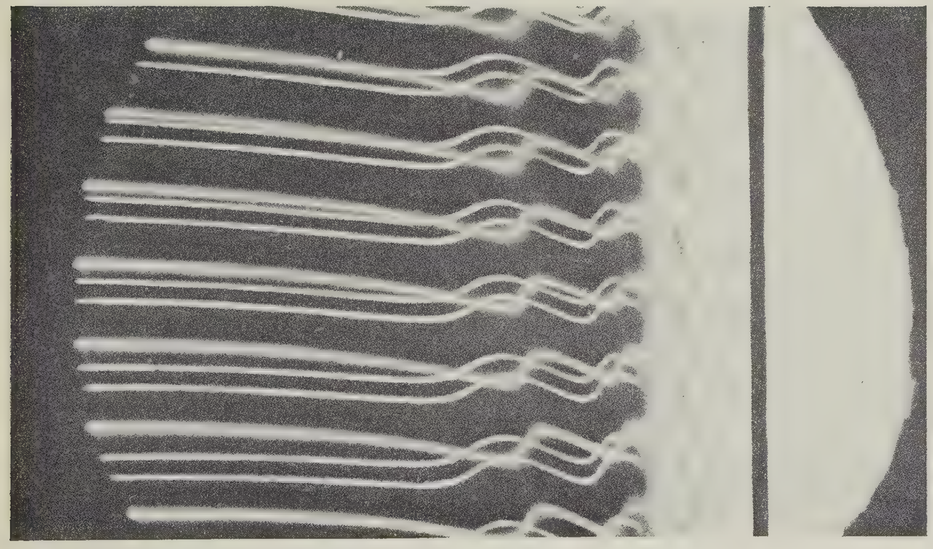

b

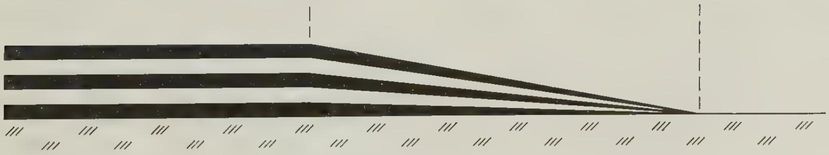

THE ORSAY 160 MeV SYNCHROCYCLOTRON WITH BEAM-EXTRACTION SYSTEM

by G. T. de KRUIFF *) and N. F. VERSTER **).

621.384.611.2

I. GENERAL DESCRIPTION
II. THE BEAM-EXTRACTION SYSTEM
III. CALCULATION AND DESIGN OF THE BEAM-EXTRACTION SYSTEM

The article below describes the 160 MeV synchrocyclotron built by Philips for the University of Paris. Special emphasis is placed on the design of a suitable beam-extraction system. After a general description of the machine in Part I, Part II deals with the operation, construction and alignment of this beam-extraction system. In Part III details are given of the method of calculation, devised by one of the authors, which enabled the builders to design the extraction system largely on paper at a time when the machine was not yet delivering an ion beam. The same method of calculation was used for the CERN synchrocyclotron at Geneva.

Introduction

Since the beginning of 1959 a synchrocyclotron built by Philips has been in operation at the Laboratoire de Physique Nucléaire at Orsay (near Paris), an institute belonging to the Faculté des Sciences of the University of Paris. The machine delivers protons of about 160 MeV or deuterons of about 80 MeV, which makes it the largest cyclotron yet built by Philips [1]) and the largest but four in Western Europe [2]).

For many investigations in the field of nuclear physics a cyclotron is a useful instrument only when the beam of fast ions which it produces can be extracted from the accelerating chamber. Although a cyclotron having only internal targets is eminently suitable for the production of neutrons and radioactive isotopes, the nuclear reactions themselves cannot properly be studied inside the accelerating chamber, where as a rule the required measuring instruments cannot be set up, where the magnetic field causes interference, and the stray radiation too — caused for example by ions incident on one of the walls — is often an insuperable obstacle. Finally, since the increase in the orbit radius per revolution is very slight, the beam can only strike the *edge* of an internal target.

The Paris cyclotron was primarily intended as a tool of pure scientific research, and therefore one of the specifications was that it should be equipped with a device to enable an ion beam to leave the accelerating chamber — a beam-extraction system. Apart from the production of an intense beam of ions, the construction of this system was the main problem to be solved. The realization of the extraction system differed from that of others operating on the same principle, inasmuch as it had to be designed and mounted before the cyclotron was delivering an ion beam with which it would have been possible to experiment. The existing theory and method of treatment therefore had to be refined. The refined treatment was first applied to the 600 MeV synchrocyclotron of the CERN at Geneva [3]); some of the necessary preliminary calculations were carried out at Philips.

In the first part of this article we give a short, general description of the cyclotron. In the second part the operation and design of the extraction system are discussed, and the third part deals with the refined mathematical treatment on which the design of the extraction system was based.

---

*) Industrial Equipment Division, Philips, Eindhoven.

**) Philips Research Laboratories, Eindhoven.

[1]) The others are all roughly the same size as the Amsterdam cyclotron (see Philips tech. Rev. **12**, 241, 247 and 349, 1950/51, and **14**, 263, 1952/53).

[2]) The four larger machines are at Geneva (CERN) 600 MeV, Liverpool 400 MeV, Uppsala 200 MeV and Harwell 175 MeV.

[3]) N. F. Verster, Symposium CERN, 1956, p. 153. See also Philips tech. Rev. **22**, 141-180, 1960/61 (No. 5), in particular note [3]) on p. 146.

I. GENERAL DESCRIPTION

A plan and side view of the whole machine (excluding ancillary equipment) can be seen in *fig. 1*. In the middle is the magnet with the accelerating chamber, on the left the radio-frequency system and the high-vacuum pumps, and on the right are the magnets for focusing and deflecting the external beam. In the plan view, the beam-extraction system can be seen at the top of the accelerating chamber, and bottom right of the chamber are the mechanisms for introducing the ion source and an internal target. The ions are made to rotate clockwise to obtain an external beam, and anti-clockwise to produce neutrons with an internal target. The change of direction is simply produced by reversing the direction of the magnetic field. The neutrons produced — most of which leave the target in the direction of the incident ions — thus move towards a part of the experiment room, adjoining the cyclotron bay, which is not occupied by equipment for proton (or deuteron) experiments. The energy of the neutrons can be varied by moving the target towards or away from the centre of the magnet. Some photographs of the equipment are shown in *figs. 2* to *5*. The principal dimensions and other data are collected in *Table I*.

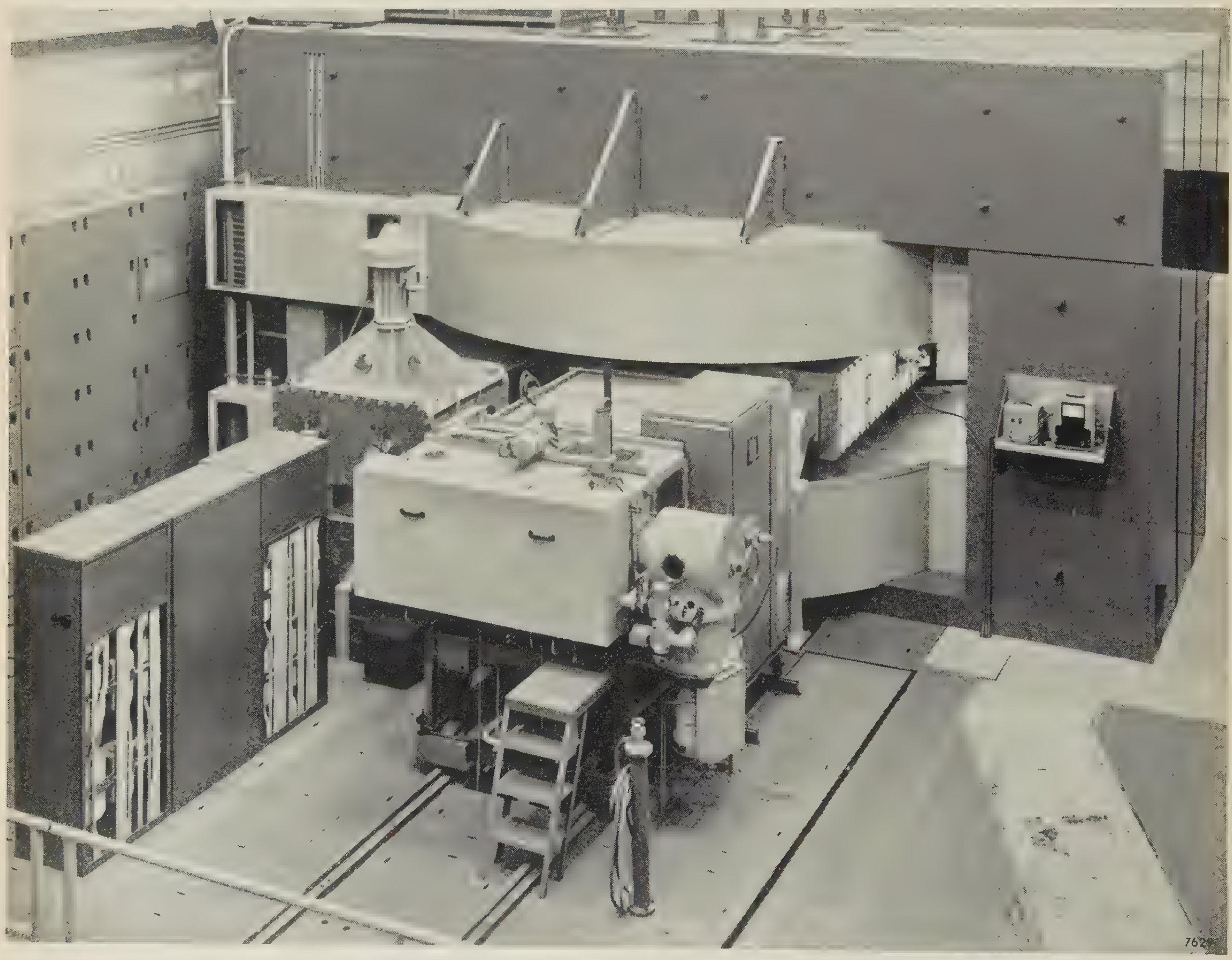

Fig. 2. The cyclotron seen from the side where the RF system is situated. The steel floor (middle foreground and left) is the roof of the large trolley (*4* in fig. 1) which carries the whole system. On the rails visible in the photograph runs the small trolley (*5* in fig. 1) which carries the modulator (centre). Right of the modulator can be seen the appertaining high-vacuum pump (Vac_3 in fig. 1) and behind it the oscillator. On the other side of the transmission line is the high-vacuum pump for the accelerating chamber (Vac_1). Behind this, visible through windows and accessible through doors, are the coil connections to the cooling-water pipe (eleven connections per coil). The three cabinets in the left foreground contain the panels for operating and regulating the water cooling. The pillar (with hose) in the foreground is connected to the general-purpose vacuum line (*7* in fig. 1).

The magnet

The poles of the magnet (diameter 280 cm) are made of circular sections 20 cm thick; to ensure a high degree of homogeneity, they were cast in vacuo, then forged and finally annealed. The yoke is assembled from 6 cm thick plates of mild steel. For our purpose the magnetic properties of this material are only slightly inferior to those of special types of steel. Except at the positions where the correction rings (shims) are mounted, the air gap is 40 cm high; at the edge, where the shims are thickest, the height is 30 cm. The induction in the air gap is about 1.6 Wb/m^2 (16 000 gauss).

The two energizing coils — one around each pole — each consist of 616 turns of aluminium tubing (24 × 24 mm; inside diameter 13 mm) through which cooling water flows. The cooling circuit is a closed system and contains deionized water. The heat is dissipated by mains water via a heat exchanger. The coils, which are connected in series, carry a current of 635 A (constant to within 0.01%). The total resistance of the coils is 1.05 Ω (at an average coil temperature of 40 °C).

Particular care was paid to the uniformity of the magnetic field. Nowhere does it differ from the required value by more than 0.0015 Wb/m^2 (15 gauss), i.e. about 0.1%, and at most places the discrepancy is in fact considerably less. The magnetic plane of symmetry coincides accurately with the geometric symmetry plane of the air gap. The relevant measurements will be discussed later in this article.

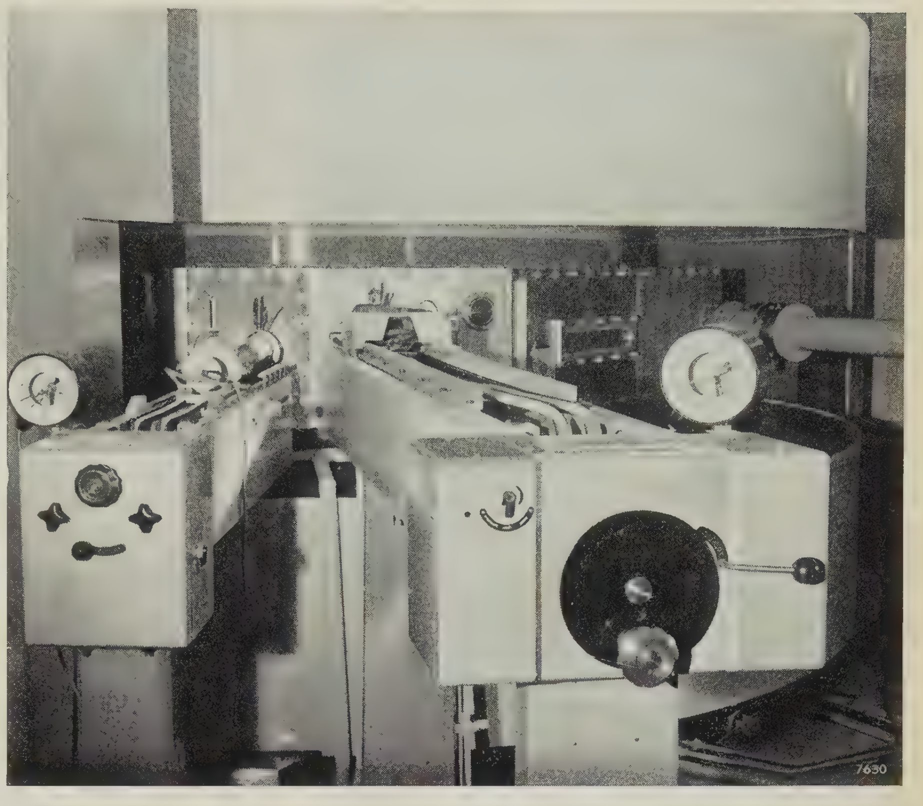

Fig. 3. Detail of the other side of the cyclotron. From left to right: the carriage for introducing a target, the ion-source carriage, window for neutron beam (in the side wall of the accelerating chamber), and the pipe for the extracted ion beam. Ion source and target are introduced in the usual way through vacuum locks. The two cabinets in the foreground contain, in addition to operating mechanisms, various locking devices. The pressure gauges indicate the pressure in the relevant vacuum lock. The vertical pipe between the two carriages is the vacuum line for the locks. The ion source is in principle identical with that in the Amsterdam cyclotron [1]).

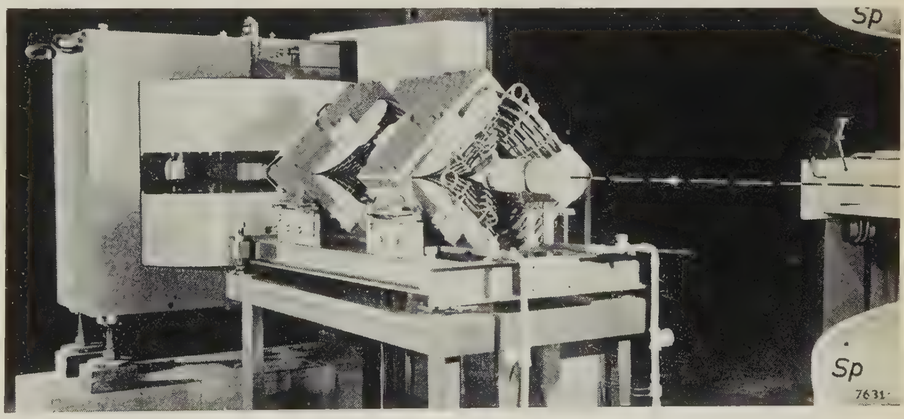

Fig. 4. The two quadrupole lenses (*2* in fig. 1) which focus the external beam, and behind them the deflection magnet (*3* in fig. 1) with which the beam can be directed to various points of the experiment room. On the extreme right are the magnet coils *Sp* of the cyclotron, and between them the ion-source carriage *I*. The communicating pipe (*1* in fig. 1) between the accelerating chamber and the lenses is missing. The centre line of the beam is denoted by dashes.

The radio-frequency system

As far as the resonator is concerned, the radio-frequency system is basically the same as in the other Philips cyclotrons. Here too the dee, the transmission line and the modulator form a coaxial resonator about half a wave in length, whose resonant frequency is determined by the capacitance of the

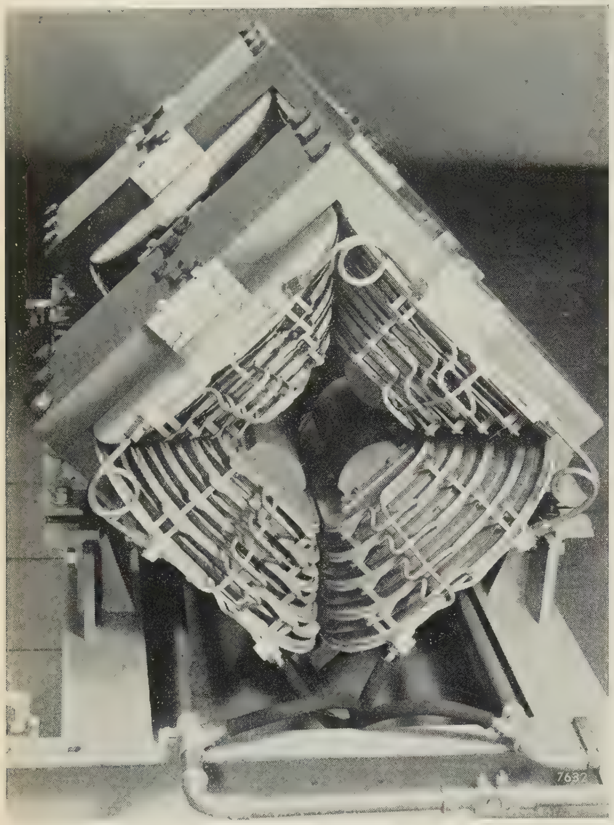

Fig. 5. The quadrupole lenses, photographed before the vacuum tube for the beam was introduced.

modulator. The dee and the modulator are at the ends of the line — at the voltage antinodes — and the coupling to the RF oscillator is somewhere in the middle. With this construction it was again possible to house the modulator in its own vacuum chamber, and as before the coupling with the oscillator could be effected at that part of the transmission line which is outside the vacuum. The modulator is of the conventional rotating type with a capacitively earthed rotor.

The diagram in *fig. 6a* represents the RF system for proton acceleration, and that in 6*b* the deuteron acceleration system. The latter can be produced from the former by wheeling the modulator back a certain distance and inserting an extra length of line between the dee and the transmission line. The modulator capacitance then has to be increased slightly with a trimming capacitor. It is not necessary to move the oscillator, steps having been taken to ensure that the distance AA' between the points where the oscillator has to be coupled to the resonator to obtain the requisite dee voltage (25 kV) in the two cases is equal to the length of the extra line section. It is thus a particularly simple matter to convert the machine from a proton cyclotron into a deuteron cyclotron.

The circuitry of the oscillator and the method of coupling the oscillator to the resonator are the same as in the CERN 600 MeV cyclotron at Geneva ("flywheel" circuit) [4]). This circuit makes it unnecessary to change the coupling in any way when switching from protons to deuterons. With an inductive coupling, as used for example in the Amsterdam cyclotron, separate loops are needed for the two frequency ranges, which makes conversion much more cumbersome.

Since, owing to the complicated form of the dee and of the feed-through insulators in the transmission line, neither the dee capacitance nor the characteristic impedance of the feed-through insulators can be exactly calculated, it is not possible to design an RF system as required in a cyclotron completely on paper. The approximate calculations were checked on a

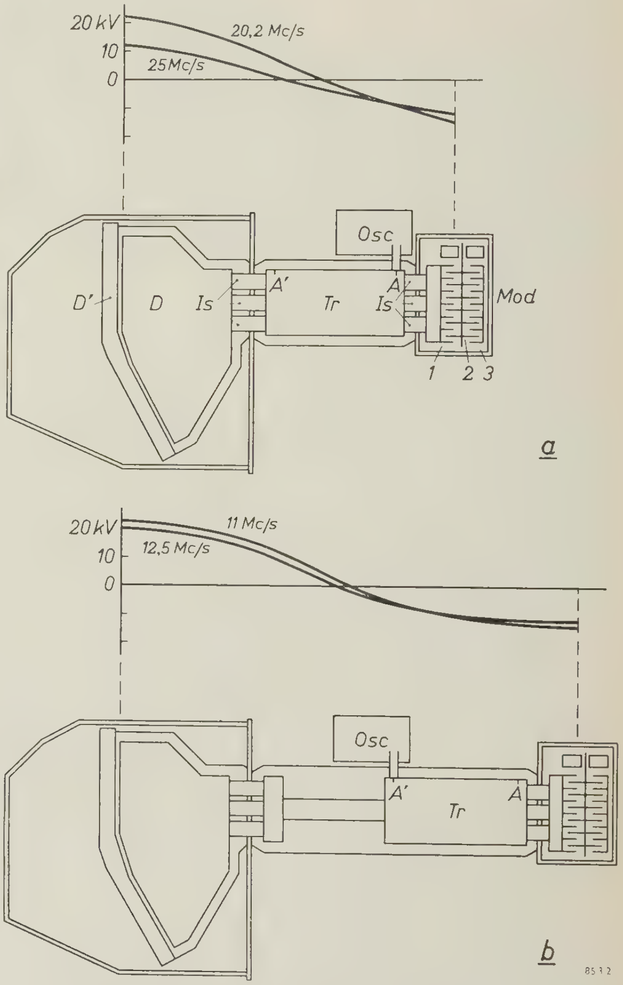

Fig. 6. Diagram of the RF system, indicating the voltage waveform across the resonator at the extreme frequency values; *a*) for proton acceleration, *b*) for deuterons. *D* dee. *D'* dummy dee. *Tr* transmission line. *Mod* modulator (*1* fixed teeth, *2* rotor, *3* earthing plates). *Osc* oscillator. *Is* feed-through insulators. The oscillator must be coupled to the transmission line at point *A* for accelerating protons, and at point *A'* for accelerating deuterons. In the conversion the oscillator can therefore stay in position. Points *A* and *A'* are situated so that at the lowest frequency a voltage multiplication of about 2× is obtained at the mouth of the dee.

---

[4]) See Philips tech. Rev. **22**, 159, 1960/61.

model (scale 1:5) and the first design improved where necessary. In order to obtain a transmission line long enough to make the above-described positioning and oscillator coupling possible, the characteristic impedance of the line had to be chosen as low as 12 Ω. The characteristic impedance of the feed-through section was kept low by using no less than three feed-through insulators in parallel at both ends.

The operation of the oscillator, in particular the coupling to the resonator, was also studied on a full-scale model. Since the maximum anode voltage of the oscillator valve (a Philips water-cooled triode type TAW 12/35) is about 12 kV, and the aim is a maximum dee voltage of about 25 kV, the oscillator is coupled to the resonator at a point where the voltage multiplication at the minimum frequency is roughly 2 (see fig. 6*a* and *b*).

The joule heat generated in the RF system is removed from the dee and the transmission line by water cooling and in the rotor of the modulator almost exclusively by radiation. To prevent the rotor getting too hot — with a view to the necessary limitation of thermal expansion — the rotor is covered with a thin layer of copper oxide. The emission coefficient is thereby increased from 0.08 to 0.65 and the operating temperature consequently lowered from about 200 °C to about 60 °C [5]).

II. THE BEAM-EXTRACTION SYSTEM

The fact that a beam of charged particles cannot usually be extracted from the cyclotron — i.e. from the magnetic field — without taking special measures, is due to the occurrence of certain instability effects. By way of explanation, and also as an introduction to the method of designing the extraction system (see Part III) we shall begin this part of the article by briefly discussing the properties of the orbit which a charged particle describes in a cyclotron.

A charged particle, of mass m and charge e, which moves in a uniform magnetic field B with a velocity v normal to the lines of force, describes a circular orbit whose radius r is proportional to the momentum mv of the particle:

$$\frac{mv}{e} = Br. \qquad \ldots\ldots \quad (1)$$

The angular velocity ω in the orbit is therefore:

$$\omega = v/r = eB/m. \qquad \ldots\ldots \quad (2)$$

If the velocity also has a component in the direction of B, the orbit is a helix.

In a cyclotron the magnetic field is not perfectly uniform but somewhat barrel-shaped (*fig.* 7). This means firstly that in the plane of symmetry the value of B decreases slightly with increasing r, and secondly that outside the plane of symmetry (assumed to be horizontal) B has a *horizontal* component B_r as well as the vertical component B_z. A particle outside the plane of symmetry is subjected to a vertical restoring force (Lorentz force) due to this horizontal component of the field. Consequently a charged particle in the cyclotron field describes vertical oscillations about the circular orbit. This vertical motion is given by:

$$m\frac{\mathrm{d}^2z}{\mathrm{d}t^2} = e\,v_\mathrm{h}\,B_r(z)\,, \qquad \ldots\ldots \quad (3)$$

where z is the distance to the symmetry plane and v_h is the horizontal component of the velocity v of the ion. In the vicinity of the symmetry plane the radial component of the magnetic induction is approximately given by

$$B_r(r,z) = z\left(\frac{\partial B_r}{\partial z}\right)_{z=0} \qquad \ldots\ldots \quad (4)$$

Further, in the air gap between the poles of the cyclotron magnet, we have curl $B = 0$. Hence:

$$\frac{\partial B_z}{\partial r} = \frac{\partial B_r}{\partial z}\,,$$

and therefore

$$B_r(r,z) \approx z\,\frac{\mathrm{d}B(r)}{\mathrm{d}r}\,.$$

(In the latter expression the abbreviated notation $B(r)$ is used for $B_z(r,0)$. Outside the symmetry plane we continue, of course, to distinguish B_z from B.) Substituting this in (3) we obtain:

$$m\frac{\mathrm{d}^2z}{\mathrm{d}t^2} = e\,v_\mathrm{h}\,z\,\frac{\mathrm{d}B(r)}{\mathrm{d}r}\,.$$

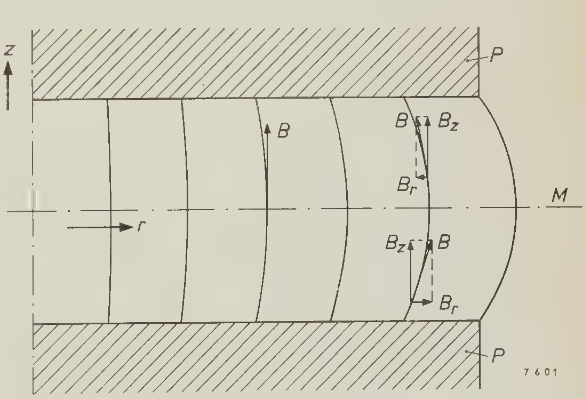

Fig. 7. Schematic representation of the cyclotron field in half the cross-section of the air gap. P magnetic poles. Outside the plane of symmetry M the horizontal component B_r of the induction is not equal to zero. In the plane M, the gradient $\mathrm{d}B/\mathrm{d}r$ is negative (cf. fig. 8).

---

[5]) This subject has been extensively investigated by G. Henneberke of Philips Industrial Equipment Division.

Provisionally we approximate to $\mathrm{d}B(r)/\mathrm{d}r$ by the value which this differential quotient has in the plane of symmetry on the circle whose radius r_0 corresponds to the momentum of the particle (cf. equation (1)). We call this circle the equilibrium orbit. Denoting the quantity $-(r/B)(\mathrm{d}B/\mathrm{d}r)$ (which is known as the field index) by n, introducing the azimuthal coordinate $\Theta = \omega t$ and disregarding the difference between v and v_h, we can reduce this equation with the aid of (1) to the very simple form:

$$\frac{\mathrm{d}^2 z}{\mathrm{d}\Theta^2} + nz = 0 . \qquad \dots\dots \qquad (5)$$

In the radial direction too, a charged particle is found to oscillate around the equilibrium orbit. The radial deviation $\varrho = r - r_0$ from the equilibrium orbit is given by:

$$\frac{\mathrm{d}^2 \varrho}{\mathrm{d}\Theta^2} + (1-n)\varrho = 0 . \qquad \dots\dots \qquad (6)$$

The method of deriving this equation resembles that used for (5).

Equation (5) and (6) have harmonic solutions, that is to say the radial and vertical oscillations of the ion are stable if $0 < n < 1$. The oscillation frequencies are respectively $\omega\sqrt{n}$ and $\omega\sqrt{1-n}$. The field index in the magnetic field of a synchrocyclotron is always positive. It increases with r but remains fairly small up to high values of r. In the fringing field of a magnet there is a marked increase in n and the critical value of unity is exceeded (*fig. 8*). This means that the ion stops orbiting and leaves the cyclotron field. The reason for this is that on the radius at which $n = 1$ the product Br has reached its maximum value, and starts to decrease with further increase in r. An ion which has been accelerated to a momentum greater than that corresponding to the maximum value of Br cannot therefore continue in a circular orbit.

This could be the basis of a very simple method of beam extraction, if in fact it were possible to accelerate an ion to the momentum mentioned. Unfortunately that cannot be done. Although, owing to our approximations, it does not appear from equations (5) and (6), the radial and vertical oscillations are not entirely independent of one another. This implies that at certain frequency ratios the one oscillation, e.g. the radial, can lose energy to the other, giving the vertical oscillation such a large amplitude that the ions are lost by collision with the dee. The smallest radius at which this effect can become serious is that corresponding to $n = 0.2$; the frequency of the radial oscillation $(\omega\sqrt{1-n})$ is then exactly twice that of the vertical $(\omega\sqrt{n})$. The next dangerous radius corresponds to $n = 0.25$. It is evident, then, that the orbit radius should not exceed the value r_c at which $n = 0.2$, for the energy gain per revolution is always fairly low in a synchrocyclotron. The orbit radius of each particle therefore increases only very slightly in each revolution (in the Orsay cyclotron about 0.1 mm at $r = 120$ cm) and thus remains very near to the dangerous value for a fairly large number of revolutions.

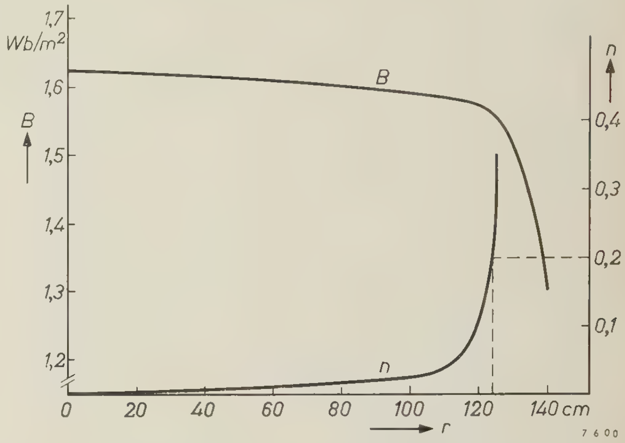

Fig. 8. Variation of induction B and of the field index n in the plane of symmetry as a funtion of distance r to the centre line of the magnetic poles. The field index reaches the critical value 0.2 at $r = 123$ cm.

Operation of the extraction system

A cyclotron beam can in principle be extracted either by means of a transverse electrostatic field or by local attenuation of the magnetic field. The first method can be used only when the energy of the ions is not too high; an impracticably high electric field strength would be required to deflect ions of 150 MeV.

In the other method of beam extraction, use is made of what is known as a magnetic channel. This is an oblong enclosure in which iron walls are used to attenuate the cyclotron field. The mouth of the channel is located between the poles of the magnet. Here the channel is perpendicular to the line connecting the mouth to the centre of the air gap. The outlet of the channel is situated outside the air gap. When an ion enters this channel, the decrease of the field causes the orbit radius to increase to a high value and the ion leaves the cyclotron field. At the outlet of the channel the ion already travels in a more or less straight line.

The difficulty of magnetic extraction is the problem of how to get the ions to enter the channel. In a synchrocyclotron it is generally speaking not possible for the channel simply to "peel off" the outermost ions from an orbiting group. The iron wall of the magnetic channel has to be many times thicker than the increase in the radius per orbit, so that the ions would land on the wall before reaching the mouth of the channel. (In the electrostatic system, on the other hand, the electrode need be no thicker than e.g. 50 μm.)

In a *regenerative extraction system* as used at Orsay, above a certain radius — which is fairly large though smaller than r_c — a forced radial oscillation is generated whose frequency gradually becomes equal to the rotational frequency of the ions. The amplitude of this oscillation increases exponentially with time, and the difference in amplitude between the ultimate and penultimate orbit is no less than, for example, 5 cm. The ions can thus enter the channel freely, provided the mouth is not too close to one of the nodes of the oscillation.

The orbit described by an ion under the influence of the extraction system can be regarded as a circle with a moving centre. At the beginning this centre precesses around that of the equilibrium orbit. Later, when the frequency of the forced oscillation is exactly equal to the frequency of rotation, it moves away quickly to one side. To a first approximation we can disregard the increase in the radius of the orbit caused by the fact that the ions continue to be accelerated during the extraction process. In the cyclotron at Orsay the circle where $n = 0.2$ has a radius of 123 cm, and that where $n = 1$ has a radius of 131 cm. The artificial generation of the required radial oscillations begins when the ion orbits have a radius of 120 cm, the channel mouth being at a distance of 133 cm from the centre.

In a regenerative extraction system the radial oscillations are generated by means of a *local* field disturbance having a marked positive gradient, i.e. in which the field increases with r; this disturbance is produced by the *regenerator*. Both radially and in azimuth the dimensions of the regenerator are small. When the orbit of an ion has a sufficiently large radius, the ion passes the regenerator each revolution. Since not only the induction in the regenerator but also the radial field gradient differs from that which the ion encounters in its orbit, the regenerator influences the state of oscillation of the ion in two ways: it alters the orbit equation (6) not only by introducing a periodic function into the right-hand side but also by causing a periodic variation in n. It can be shown that this is the reason why the frequency of the forced oscillation ultimately becomes *exactly* equal to the orbital frequency of the ions [6].

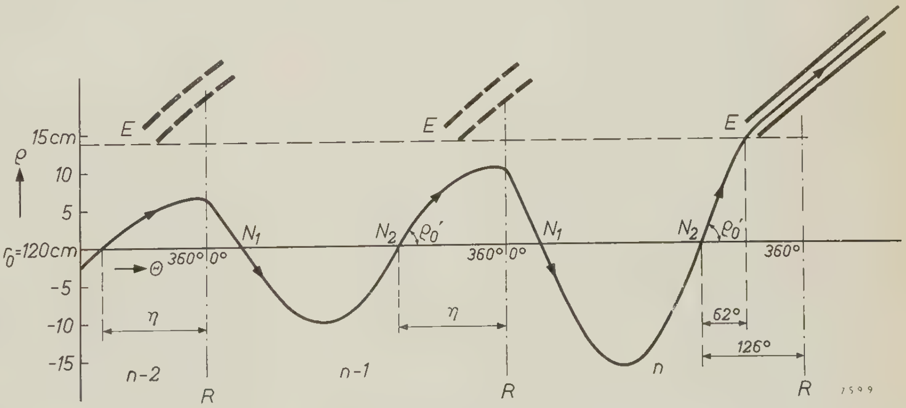

Fig. 9. Principle of beam extraction with a regenerative extraction system. The radial deflection ϱ of an ion, measured from the equilibrium orbit, is plotted as a function of azimuth Θ for the last revolutions of the ion (orbit number n, $n-1$, $n-2$). The regenerator is located at R, where it produces a field with a steep positive radial gradient; its azimuth is taken as zero. E mouth of magnetic channel. N_1 and N_2 penultimate and ultimate passage of the ion through zero in each revolution before reaching the regenerator. In the extraction system as designed, the azimuth difference η between N_2 and R has the same value in each revolution. The amplitude of the oscillation increases to such an extent during the last revolutions that the ion in orbit $n-1$ still misses the channel by a considerable distance. The azimuth differences indicated refer to the actual extraction system.

The amplitude of the vertical oscillations is kept within limits with a second local field disturbance, in which the field has a strong *negative* gradient. In older cyclotrons using magnetic beam extraction, this field disturbance was produced with the aid of a steel construction known as a peeler [7]. In the cyclotron under consideration the region of negative gradient is not obtained artificially but by using the fringing field. Although this is not in fact a local field disturbance, it amounts to that as far as radially oscillating ions are concerned: these enter the fringing field only in a limited part of their orbit.

Since the behaviour of an ion in a magnetic field is governed solely by its momentum, i.e. by the product Br, ions of all kinds behave in the same way in the cyclotron field on a circle having a specific radius; protons and deuterons can therefore be extracted by one and the same system.

Fig. 9 gives a qualitative illustration of the positioning of regenerator and channel and the path described by an ion on its last orbit. Depending on the current, the intensity of the external beam is 5 to 12% of that of the internal beam (Table I). The remainder of the internal beam falls on a water-cooled diaphragm mounted at the mouth of the channel; this diaphragm also serves as a target for the production of radioactive isotopes with a long half life.

---

[6] This method was first successfully applied in the Liverpool cyclotron. We acknowledge here our indebtedness to the late Professor Skinner and to Dr. V. Moore for the hospitality they showed us on our visits to the Nuclear Physics Research Laboratory of Liverpool University, to Dr. K. J. Le Couteur, who allowed us to see one of his articles before publication, and to Dr. A. V. Crewe for many useful discussions.

[7] Although the names regenerator and peeler are not a fortunate choice, we shall conform to general usage in this matter.

This form of the regenerative method of extraction, which was proposed and treated theoretically by Le Couteur and Lipton [8]) in 1955, has two advantages over the system using a peeler [9]). In the first place a peeler is more difficult to make than a regenerator. Moreover, when a peeler is used the deflection has to be effected in a region where the field gradient is practically constant, i.e. at an appreciably smaller distance from the centre than half the pole diameter of the magnet. The ions can therefore not be accelerated to the maximum possible energy (i.e. the energy at which the orbit coincides with the circle where $n = 0.2$). It might be regarded as a disadvantage of the method not using the peeler that its mathematical treatment is more difficult and leads to equations that can only be solved numerically (see Part III). It is equally true, however, that excellent insight is obtained in this way into the behaviour of the ions.

Construction of regenerator and magnetic channel

Owing to the manner in which, for various reasons, the cyclotron had to be sited in the space available, a restriction was imposed on the direction of the external beam: the angle between that direction and the principal axis of the cyclotron could not be greater than 30° (cf. fig. 1). This requirement could only be satisfied by having a relatively long magnetic channel which would quickly remove the beam from the influence of the magnetic field. The form and situation of this channel have already been broadly indicated in fig. 1. A more detailed plan view being given in *fig. 10*.

The channel consists of nine segments, the length of which increases as the curvature of the orbit decreases: the segment at the mouth is the shortest and that at the outlet the longest. Most of the segments consist of two thick vertical iron plates, mounted in the plane of symmetry of the cyclotron at either side of the path which the beam has to follow. Some segments consist of only one such plate.

Since of course the field is reduced on *both* sides of the plates, they also disturb the cyclotron field outside the channel. This disturbance imposes certain limitations on the field reduction that can be achieved in the first segments, and measures are needed to correct for it as far as possible. This is done with the aid of iron correction plates which are mounted in pairs in the accelerating chamber — this time above and below the plane of symmetry and far enough away from it to avoid obstructing the ions. The field

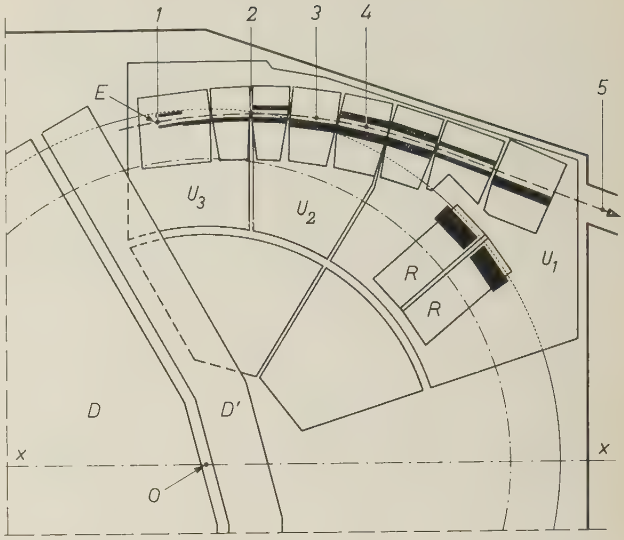

Fig. 10. Positioning in the cyclotron of the regenerator and of the nine segments that together form the magnetic channel (see fig. 1). *O* centre point of magnet poles. The outer circle represents the edge of the magnet poles. *x-x* principal axis of the cyclotron. *D* dee. *D'* dummy dee. U_1, U_2 and U_3 aluminium plates on which the regenerator and the channel segments are mounted. *R* regenerator, consisting of two parts. *E* inlet of first channel segment. The dot-dash circle is the equilibrium orbit on which the deflection begins ($r = 120$ cm). The external beam makes an angle of less than 30° with the *x-x* axis. The significance of the numbers *1* to *5* is explained in fig. 12.

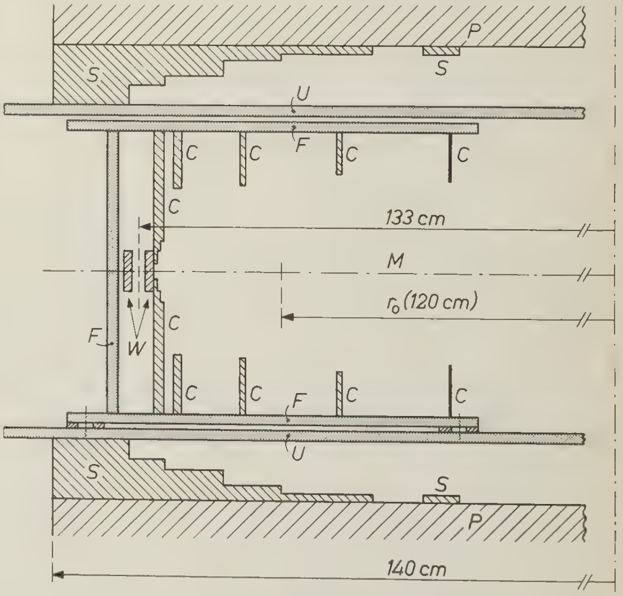

Fig. 11. Method of assembling the steel walls *W* of one segment of the magnetic channel, here the first segment, with the appertaining steel correction plates *C*. *P* the two magnet poles. *M* plane of symmetry. *S* shims. *U* aluminium plates, fixed to *P* and S, to which the *U*-shaped aluminium frame *F* is secured. This frame carries both the channel walls and the correction plates.

---

[8]) K. J. Le Couteur and S. Lipton, Phil. Mag. **46**, 1265, 1956.

[9]) J. L. Tuck and L. C. Teng, Phys. Rev. **81**, 305, 1951. A mathematical treatment will be found in: K. J. Le Couteur, Proc. Roy. Soc. **A 232**, 236, 1955.

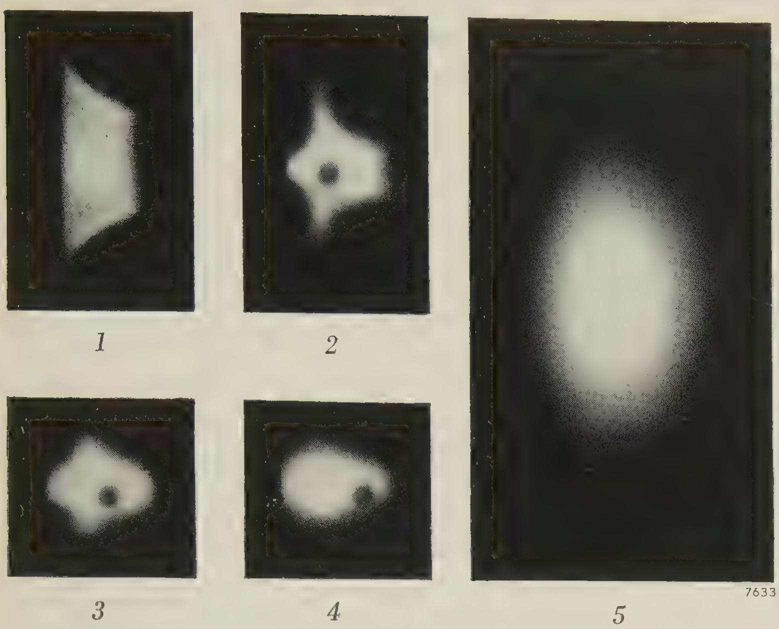

Fig. 12. Cross-section (true size) of the proton beam in the magnetic channel at the points indicated by *1* to *5* in fig. 10. The figures are autoradiographs, obtained by keeping a copper plate at the places mentioned for a few seconds until it became radioactive and then laying it on photographic paper. The spots visible in *2*, *3* and *4* indicate the middle of the channel.

reduction brought about by the segment plates is relatively greater nearby and relatively smaller at a considerable distance away, as the height of the segment plate decreases. The segment plates should therefore not be made too high.

The plates of each segment and the pertaining correction plates are mounted on a U-shaped aluminium frame as illustrated in *fig. 11*. The frames themselves are mounted on three horizontal aluminium plates — the first two carry three segments and the last one three segments plus the regenerator — which are secured to the bottom pole face of the magnet: on the outside they rest directly against the shims, which give the fringing field the appropriate pattern, and on the inside they rest on studs. Similar plates (ceiling plates) are also mounted above the frames on the upper pole face of the magnet; the frames are fixed to these plates so that they can better withstand the large radial forces acting upon them in the strong cyclotron field. The whole assembly is designed in such a way that during check measurements (see following section) changes can quickly be made to the channel mouth and the correction plates.

Table II. Principal data of magnetic channel. The segments are numbered in the sequence in which they are traversed by the ions.

Segment	Length mm	Thickness inside wall mm	Thickness outside wall mm	Width mm	Height mm	Field drop 10^{-4} Wb/m^2	Gradient 10^{-6} Wb/m^3	Type of steel
I	100	7.5	7.5	12	35	—3100	—1490	cobalt steel
II	100	10.0	—	—	37.5	— 800	— 186	,,
III	150	12.5	—	—	40	—1375	— 62	,,
IV	150	15.0	15.0	15	40	—5450	—1140	,,
V	200	25.0	—	—	40	—3760	+1211	,,
VI	200	30.0	30.0	20	60	—6040	— 727	mild steel
VII	200	30.0	30.0	20	60	—	— 640	,,
VIII	250	25.0	15.0	30	60	—	+ 60	,,
IX	250	35.0	—	43	80	—	+ 380	,,

Just as the channel walls disturb the cyclotron field, so too do the correction plates, which are intended to eliminate this effect, disturb the field in the channel: this causes a further increase in the (radial) field gradient, which is already quite large here. The consequence in the channel is a focusing effect in the vertical plane and a defocusing effect in the horizontal plane. To eliminate the latter effect, four segments have only a single wall, the outer wall being omitted. The field gradient in these segments is considerably less negative or even positive. The result is a channel that can be regarded as a system of magnetic lenses which alternately focus and defocus in the horizontal plane, and do just the reverse in the vertical plane. The field reduction is of course appreciably lower in the single-walled segments than in the others. The principal data relating to the nine segments are summarized in *Table II*. *Fig. 12* shows the cross-section of the beam at various points in the channel.

It will be clear, having regard to the complexity of the whole assembly, that the final form of the channel (including the correction plates) was not achieved entirely without trial and error. We shall return to this point presently.

A cross-section of the regenerator can be seen in *fig. 13*. The regenerator field is produced with the aid of the steel blocks *R*, the plates *C* on the right again

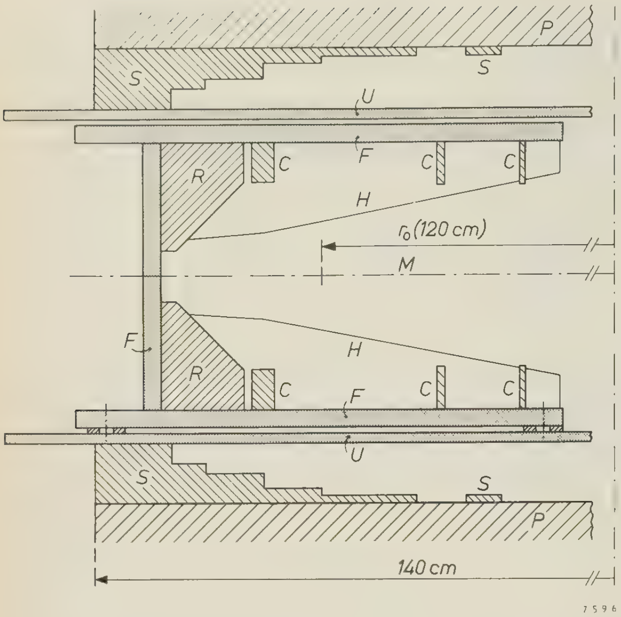

Fig. 13. Schematic cross-section of one of the regenerator halves. *P* and *S* are again respectively the magnet poles and shims. The regenerator field is produced by means of the steel blocks *R*. The blocks and plates *C* again have a corrective function. *R* and *C* are mounted in the same way as the channel segments (see fig. 11), except that the construction is reinforced by two ribs *H*. Dimensions of the four blocks *R* are: 200 mm long, 75 mm wide, 97.5 mm high outside and 37.5 mm high inside.

being correction plates. The mechanical design resembles that of the channel segments. Two reinforcement ribs *H* are fitted to the centre of the frame, one above and one below, to enable the system to withstand the powerful radial forces which act on the steel blocks in the very inhomogeneous boundary field. A set of regenerator blocks and correction plates as shown in fig. 13 is mounted on each side. The two sets are at an angle of 7° to one another in the horizontal plane, so that the shape of the regenerator is adapted somewhat to that of the ion orbits. The whole assembly can be displaced radially. A general view of the channel and regenerator is to be seen in *fig. 14*.

The field disturbances encountered by an ion passing the regenerator in an orbit of radius 127 cm are represented in *fig. 15*.

Field correction and alignment of the extraction system

For applying the field corrections presently to be discussed, and in aligning the channel and regenerator, use was made of a light, flexible copper wire which acted as an "orbit simulator" [10]). With refer-

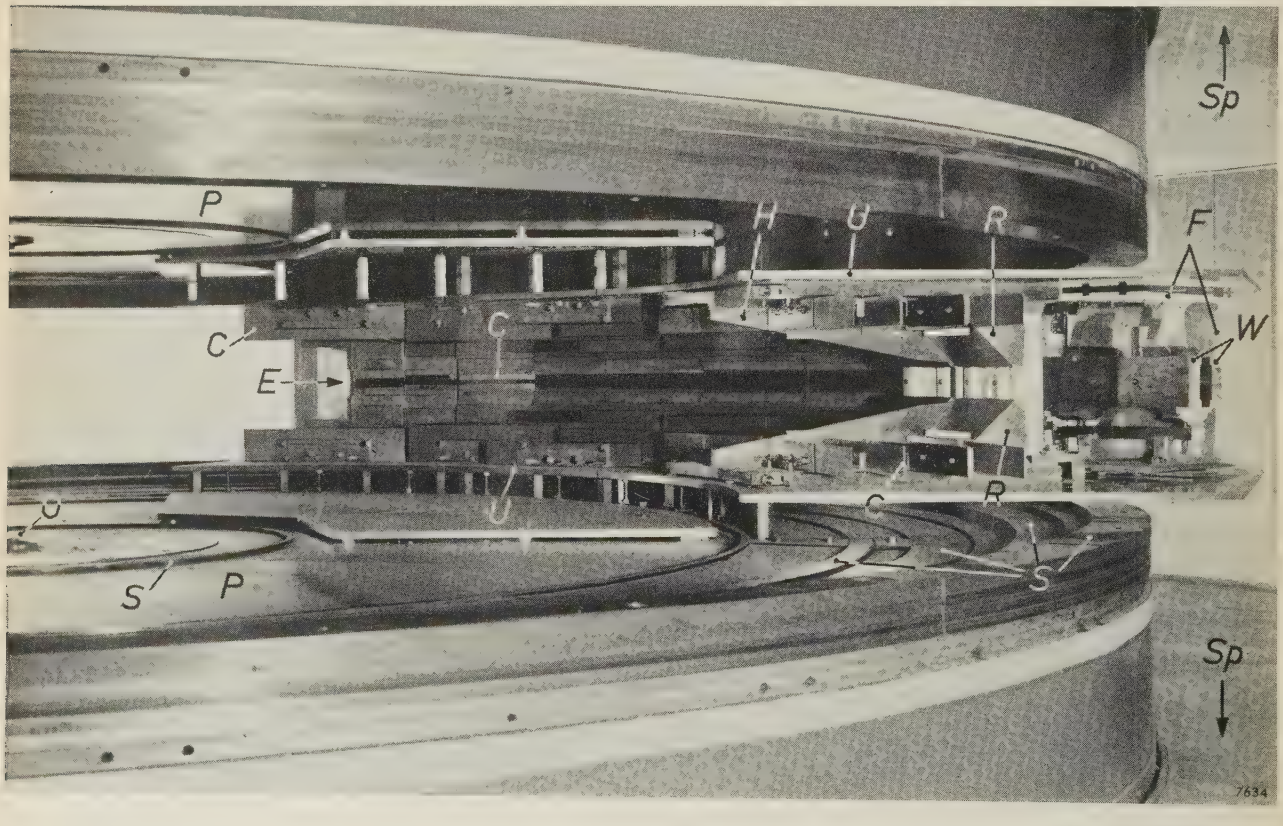

Fig. 14. The extraction system, photographed when the cyclotron was under construction. The letters have the same meaning as in figs 10, 11 and 13. On the far right can be seen the walls *W* of the last channel segment (in the final alignment the outer wall of this segment was omitted, see Table II). The walls of the segments *I* to *VII* can be seen on the left of the regenerator *R* as dark patches between the correction plates *C*.

---

[10]) See G. R. Lambertson, UCRL 33-66.

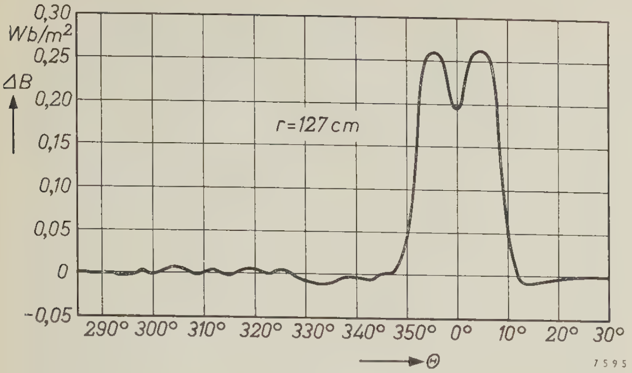

Fig. 15. The difference ΔB between the induction B in (and around) the regenerator and the average value of B outside the regenerator on a circle of 127 cm radius. The abscissa is the azimuth Θ of the points of the circle.

ence to *fig. 16* we shall first briefly examine the principle of this method.

In this figure the curve represents the conductor, assumed to be perfectly flexible. It is rigidly secured at points X and Y. The lines of force of the field B are perpendicular to the plane of the drawing. In this plane each element Δs of the wire is subjected to a Lorentz force of magnitude $IB\Delta s$ perpendicular to the direction of I. In the equilibrium state the shape of the wire is such that this force on each element is equal and opposite to the radial component $K\Delta a$ of the mechanical strain K in the wire:

$$K\Delta a = -IB\Delta s\,.$$

Now $\Delta s = r\Delta a$, so that this formula can be reduced to $K/I = -Br$. It follows, then, that the shape of the wire is such that the product Br has the same value at every point, for K and I have the same value at every point.

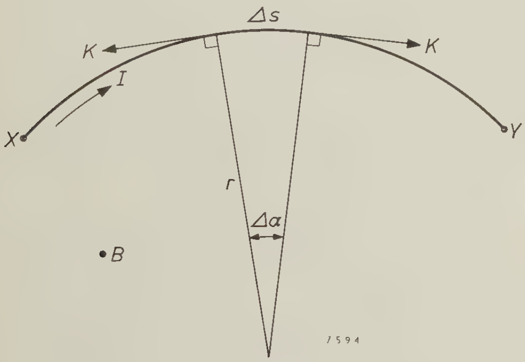

Fig. 16. Illustrating the use as an "orbit simulator" of a copper wire fixed between two points X and Y.

The same also applies, however, to the orbit of an ion (eq. 1), for the product Br is proportional to the momentum. The wire thus gives us at once the form on any particular ion orbit. If *three* points of an orbit are known, I and K need not be measured at all; it is then only necessary to make the wire long enough to pass the third point. The two extreme points are here again the fixed points, and the length is adjusted until the wire also passes through the third. If a sufficiently large current is chosen, the weight of the wire can be disregarded.

We used a hard-drawn, enamelled copper wire of 0.25 mm diameter and a current of 3 A. If the orbit of a 157 MeV proton in the cyclotron field is simulated in this way (at a B value of 1.57 Wb/m^2 the radius is 120 cm), the tension in the wire is about 6 newton.

It should be noted that the Lorentz force acting on an element of the wire is opposed to that which acts on a moving ion. Outside the plane of symmetry the vertical component of this force repels the wire away from this plane instead of attracting the wire towards it, as in the case of an ion. A freely suspended wire would thus be vertically unstable. We shall return to this point when discussing the various applications.

Field corrections

The field corrections made using the orbit simulator method were 1) a symmetry-plane correction and 2) a centre-point correction.

In designing the extraction system it was assumed that the magnetic plane of symmetry, in which the equilibrium orbits of the ions lie, coincides with the geometric plane of symmetry. In fact, however, no matter how carefully the magnet and coils are made, this may not be the case. The manner in which this was investigated in the present cyclotron is sketched in *fig. 17*. The ends of the wire are fixed to a vertical pin attached to a float. The wire can thus move freely in the horizontal plane. If necessary, the level of the water in which the assembly floats can be altered slightly. To prevent

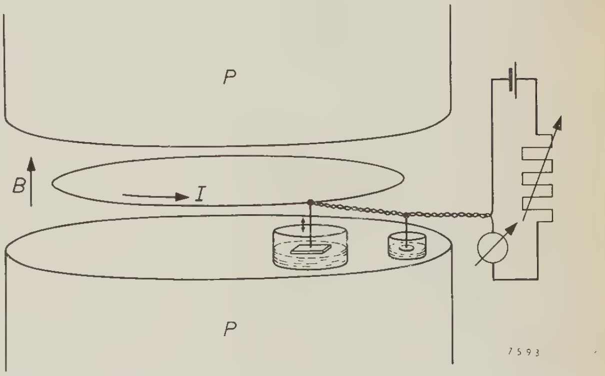

Fig. 17. Diagram illustrating the use of the orbit simulator for finding the magnetic plane of symmetry and the centre of the cyclotron field. The two ends of a wire, which forms a full circle, are here attached to a pin set up vertically on a float. When the point of adjustment is in the plane of symmetry, a variation in I has no influence on the impression of the float in the water. In the horizontal plane the wire conductor can move freely. It takes up a position on a circle which is concentric with the magnetic centre of the cyclotron field.

the wire being influenced by radial forces that do not in reality act on an ion, the supply line is twisted and attached to a second float.

By mounting the wire on a float we have eliminated the vertical instability which, as just noted, would attach to a freely suspended wire, while at the same time retaining some vertical mobility. The position of the symmetry plane at the point of suspension of the wire is now found by determining that level of water in the vessel at which a change in the current I through the wire does not influence the vertical position of the float. If the wire is outside the symmetry plane, an increase of I will shift the equilibrium position to a point still further removed from this symmetry plane. The entire plane of symmetry can be charted by performing measurements of this kind at numerous points.

This procedure revealed that the magnetic plane of symmetry was initially somewhat curved. It coincided with the geometric symmetry plane near the centre, but at a radius of 120 cm it was 12 mm above it. Especially in view of the limited height of the channel mouth (about 40 mm) this was unacceptable. The trouble was corrected by compensating the asymmetry in the iron core of the magnet with an opposite asymmetry in the coils. For that purpose the lower coil was shunted with a resistance of 15.5 Ω, causing a current of 635 A to flow through the upper coil and 615 A through the lower coil. In this way the discrepancy was reduced to less than 2 mm.

The centre-point check, which we shall now discuss, shows whether the centre of an ion orbit coincides with the geometric centre of the magnet. Plainly, this can also be investigated using the set-up in fig. 17. Discrepancies occur when a cyclotron field is not azimuthally homogeneous. In a cyclotron with a regenerative extraction system, inhomogeneities are due to regenerator and the channel: before correction, their effects are perceptible down to quite a small radius. The presence of such inhomogeneities is undesirable. They tend to give rise to radial oscillations — as in the regenerator — and therefore have an adverse effect on the intensity and energy distribution of the external beam. Ions that describe large radial oscillations may well come under the influence of the regenerator too soon and be extracted before they have reached the energy that corresponds to an orbit radius of 120 cm.

The check was carried out by successively determining the radial position of four points in pairs diametrically opposite to one another. The discrepancies were corrected by locally increasing the induction with the aid of thin plates (1 mm thick) secured symmetrically with respect to the plane of symmetry to the upper and lower poles. The magnetic centres of orbits having a radius between 30 cm and 115 cm are now less than 1 cm from the geometrical centre of the magnet.

Alignment of magnetic channel and regenerator

To find the definitive position of the magnetic channel (*fig. 18*) one end of the wire conductor was fixed to the circle with $r = 120$ cm at the calculated penultimate node N_1 (cf. fig. 9) of the orbit terminating at the channel. The other end was passed through the provisionally mounted channel and attached some distance outside it to a point which we shall call Z. The length was adjusted so that the wire passed the calculated ultimate node N_2. The position of Z was chosen so that the line between Z and the outlet of the channel satisfied the abovementioned requirement that the external beam should make an angle of at most 30° with the principal axis of the cyclotron.

Next, the position of the channel was adjusted until the wire passed precisely through its middle. By shifting the point Z towards either side so that the wire only just failed to make contact with the walls of the magnetic channel (see dashed lines in fig. 18) it was possible to determine which part of the ion beam entering the mouth of the channel

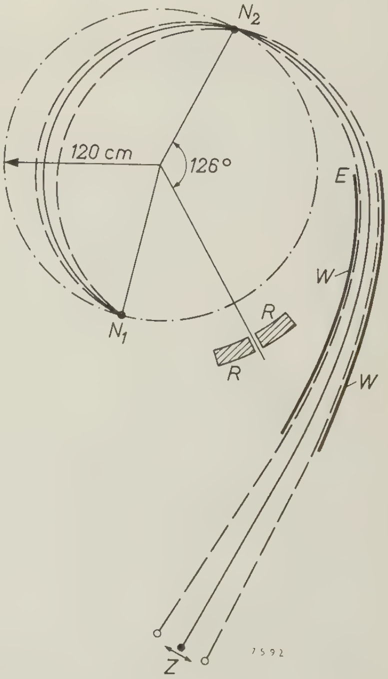

Fig. 18. Finding the optimum position of the channel W by means of the orbit simulator. The ends of the wire are secured at the calculated penultimate node N_1 of the orbit described by the ions, and at an external point Z. The length was adjusted so that the wire passed through the calculated last node N_2.

reaches the outlet, and also the horizontal divergence of the external beam. Originally only the fifth segment of the magnetic channel was single-walled. Calculations — confirmed by the measurements with the orbit simulator — showed that with this configuration only a 1.5 mm wide part of the beam entering the mouth of the channel would reach the outlet. As mentioned, the radial defocusing in the magnetic channel, which was responsible for the poor result, is substantially reduced by also making segments *II*, *III* and *IX* single-walled (see Table II). The consequent decrease in the deflection made it necessary to situate the mouth of the channel 2 cm further outwards. The simulator measurements now showed that an 8 mm-wide portion of the beam incident on the channel mouth would reach the outlet of the channel. Considering that the channel mouth itself is only 12 mm wide, this is a highly satisfactory result.

Two different check measurements were made with the orbit simulator to determine the optimum position of the regenerator. The first was intended to investigate whether the generation of the forced oscillations with increasing amplitude in fact began at a radius of 120 cm. To this end, use was again made of a closed wire loop, length $2\pi \times 120$ cm, mounted on a float (cf. fig. 17). The wire was set up in the cyclotron field and the regenerator moved as far as possible away from the middle. The regenerator was then moved (radially) inwards and the position was accurately determined at which the wire became unstable. We call this position R_1.

The second measurement was made with the wire arrangement illustrated in *fig. 19*. This differs from fig. 18 only inasmuch as the "internal" fixed end had been shifted towards a point L in front of the regenerator, situated on the calculated orbit of an ion which describes the path (through N_1) shown as a solid curve in fig. 18 ($\Theta = -27.5°$, $r = 128.8$ cm; the azimuth angle Θ was measured from the regenerator). To start with, the regenerator was moved as far as possible outwards, and the length of the wire adjusted so that the nodal points N_1 and N_2 were passed at equal distances (on the inside and outside respectively). Next, the regenerator was moved inwards and the position was determined at which the wire cut the equilibrium orbit $r = 120$ cm exactly at N_1 and N_2. Since the channel position corresponding to N_1 and N_2 had already been found (see above), the wire then runs automatically through the middle of the channel. We call this position of the regenerator R_2

It was found that the regenerator positions R_1 and R_2, and the previously calculated position used for applying the correction plates, differed by less than 1 millimetre.

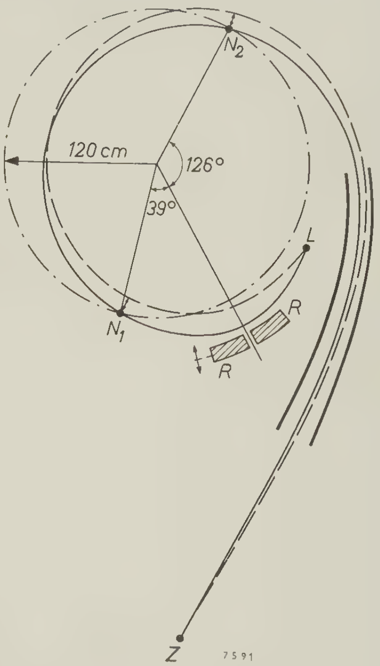

Fig. 19. To find the correct radial position of the regenerator R, the internal fixed end of the wire was set at point L ($\Theta = -27.5°$, $r = 128.8$ cm) situated on the calculated orbit of an ion that follows, starting from N_1, the path shown as a full line in fig. 18. The regenerator was moved from outside inwards until the wire passed through the nodes N_1 and N_2.

Finally, *fig. 20* shows an autoradiograph of the cross-section of the external beam (in this case a proton beam) 3 metres behind the outlet of the extraction system.

Nature of the external beam

If no special measures are taken, the current of the accelerated ions delivered by a synchrocyclotron is not continuous but consists of short pulses, the interval between which is equal to the oscillation period of the modulator. In the present cyclotron the length of these pulses is about 25 μsec and the interval between them is about 2200 μsec; this means that the current in the pulses is about 100 times stronger than the average current.

After completion of this cyclotron, Dr. A. Cabrespine (University of Paris) fitted an auxiliary device which "spreads" the pulses so as to produce a more or less continuous ion current [11]. In this way the maximum count rate to be handled by the counting equipment used in the investigations is appreciably reduced, causing a decrease in the fraction of particles (or quanta) *not* counted and

---

[11] See A. Cabrespine, J. Phys. Radium **21**, 332, 1960. This method of spreading out the pulses is based on an idea of R. Keller (Int. Conf. on high energy accelerators and instrumentation, CERN, 1959, p. 187).

Fig. 20. Autoradiograph (true size) of the cross-section of the external proton beam, three meters behind the exit of the extraction system. The quadrupole lenses (*2* in fig. 1) were not in operation when this autoradiograph was made.

also in the number of random coincidences in coincidence measurements. As a result the precision of the measurements is increased and the duration of the measurements can be considerably shortened. The method of spreading out the pulses is as follows.

The oscillator is switched off during that part of each modulation period in which the frequency would pass through the range of minimum values, and in this way the ions are accelerated to an energy which is not quite sufficient to bring them under the influence of the regenerator. Instead of being extracted, they thus continue revolving in the last orbit reached, and after a short time they populate the entire periphery. When the accelerating voltage is switched off, there is no longer any phase stability and the effect of small differences in energy is soon felt. The energy which the ions still lack in order to be extracted is imparted to them by means of an auxiliary electrode. (In figs. 1 and 10 this should be drawn near the right side wall of the accelerating chamber between the regenerator and the ion-source carriage.) This electrode is connected to a low-power RF generator whose average frequency is equal to the average value of the frequencies which the large generator would otherwise have swept during the quiescent period. The frequency of this small generator is very rapidly modulated (for example, modulation frequency 30 000 c/s and frequency sweep 300 kc/s). As a result of this very rapid frequency modulation, combined with the fact that the ions no longer revolve as a group but are uniformly distributed over the entire periphery, during every frequency sweep (of the small generator) only a small fraction of the ions which together would otherwise have delivered a single pulse is accelerated to the energy at which extraction is possible. Remarkably enough, this process can be continued for some time after the main generator has again been switched on and has started to accelerate a succeeding group of ions: the pulse can thus in fact be spread out. Depending on the circumstances, the average intensity of the beam in this process is 20 to 25% of what would otherwise be obtained.

III. CALCULATION AND DESIGN OF THE BEAM-EXTRACTION SYSTEM

In view of the large radial amplitudes that occur in the last phase of the extraction, we used in our design of the beam-extraction system not only the equations (5) and (6), mentioned in Part II, but also, where necessary, the more accurate equations:

$$r'' = -r\frac{rB - r_0 B_0}{r_0 B_0} = -\frac{r}{r_0}\left(r - r_0 + r\frac{B - B_0}{B_0}\right), \qquad (7)$$

$$z'' = z\frac{r^2}{r_0 B_0}\,\frac{\mathrm{d}B}{\mathrm{d}r}. \quad \dots\dots\dots \quad (8)$$

Here B_0 is an abbreviated notation for $B(r_0)$ and $r'' = \mathrm{d}^2r/\mathrm{d}\Theta^2$ etc. The main difference compared with equations (5) and (6) is that B in this case is not approximated by $B_0 + (\mathrm{d}B/\mathrm{d}r)(r - r_0)$. If the amplitude is allowed to approach zero, equations (7) and (8) reduce to (5) and (6).

Equations (7) and (8) are entirely adapted to the situation that arises during the extraction: the amplitude of the radial oscillations then increases considerably whilst that of the vertical oscillations remains small. As can be seen, the coupling between the radial and vertical oscillations, which was not included in (5) and (6), is now taken into account in the equation for the vertical oscillation — r appears in (8) and cannot be approximated by r_0 — but not in that for the horizontal oscillation. The neglect of the influence of the vertical oscillation on the horizontal is an essential feature of the method of calculation discussed in this part of the article. Numerical computations which did allow for the latter influence have shown that this neglect is permissible.

Since the dimensions of a regenerator in the orbital direction are small compared with the wavelength of the oscillations described by the ions, the regenerator in our calculations is replaced by an equivalent infinitely thin regenerator. Its strength can be characterized by a function I which depends solely upon r:

$$I(r) = \int \frac{\Delta B}{B_0} r_0 \mathrm{d}\Theta . \quad . \quad . \quad . \quad . \quad . \qquad (9)$$

Here ΔB is the difference between the field inside the regenerator and that outside it, both at a radius r. Assigning to the regenerator the azimuth $\Theta = 0°$ and giving symbolically the quantities directly in front of the regenerator the coordinate $-0°$ and those behind it $+0°$, we can find by integration from (7) and (8) that the radial motion for every passage of an ion is given by

$$r(+0) = r(-0) , \quad . \quad . \quad . \quad . \quad . \quad . \quad . \qquad (10a)$$

$$r'(+0) = r'(-0) - \left(\frac{r}{r_0}\right)^2 I(r) , \quad . \quad . \qquad (10b)$$

and the vertical motion by:

$$z(+0) = z(-0) , \quad . \quad . \quad . \quad . \quad . \quad . \quad . \quad . \qquad (11a)$$

$$z'(+0) = z'(-0) + z \left(\frac{r}{r_0}\right)^2 \frac{\mathrm{d}I}{\mathrm{d}r} . \quad . \qquad (11b)$$

We shall first briefly illustrate how the orbit of an ion can be found when the function $I(r)$ is known, after which we shall discuss how, conversely, starting from a required form of orbit, we designed a suitable regenerator.

In computing the behaviour of an ion in a cyclotron with a regenerative beam-extraction system, we divide the history of the ion into four periods:

a) The period in which the ion is accelerated in the normal way.

b) The period in which, under the action of the regenerator, the free oscillations become forced oscillations. The amplitudes are still small. This period has an important bearing on the spread in the energy of the extracted ions [12]).

c) A period in which the amplitude of the forced oscillations, while still being small, is nevertheless already too large for one to be able to use equations (5) and (6). Periods *b* and *c* together comprise a large number of revolutions.

d) The last period before the ion enters the magnetic channel. In this period, which comprises only a few revolutions, the amplitude rapidly increases (cf. fig. 9). Accurate analysis of this period is particularly necessary to the design of an effective regenerator and the magnetic channel.

We shall now examine the behaviour of an ion during periods *c* and *d*, dealing separately with the radial and the vertical oscillations. We begin with period *d*, and assume for the moment that we know the state of oscillation at the end of period *c*.

We describe the radial behaviour (outside the regenerator) of an ion on an orbit with "equilibrium radius" r_0 by the variation of the deviation $\varrho = r - r_0$ along the orbit. For period *d* we find this, using an electronic computer, by solving equation (7) for the measured variation of $B(r)$ around $r = r_0$ and for a chosen value of the amplitude $\varrho_{\max}$. It is simpler here to take as our starting point not the amplitude $\varrho_{\max}$ itself but the slope ϱ_0' of the orbit in relation to the equilibrium orbit at the point where these intersect. Examples of such solutions for this cyclotron are given in *fig. 21*. It can clearly be seen that the small-amplitude oscillation is almost sinusoidal, but that the large-amplitude one is not. The outward deflections, bringing the ion into the fringing field, are larger and last longer than the inward deflections. In fig. 21 the azimuth coordinate used is not the angle Θ with respect to the regenerator but the angle ψ with respect to the last point N_2 where the ion passes through zero before reaching the regenerator (cf. fig. 9). We shall use this azimuthal quantity in all our subsequent calculations. The ψ values of the regenerator at the beginning and end of a revolution are denoted as η and $\eta + 360°$. The angular position of the oscillation with respect to the regenerator will be characterized by this angle η, which for convenience we shall refer to as the "phase" of the oscillation (cf. fig. 9).

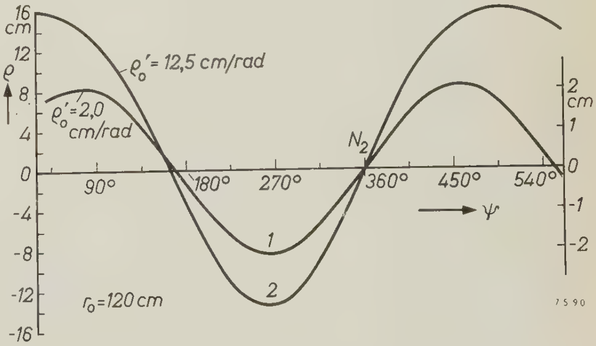

Fig. 21. Solutions of the radial orbit equation for orbits having an equilibrium radius of 120 cm. In orbit *1*, ϱ_0' is small (2 cm/rad), in orbit *2* it is large (12.5 cm/rad). In orbit *1* the ion does not enter the fringing field; the oscillation is almost sinusoidal. In orbit *2* there is marked asymmetry: the deflection outwards is greater than that inwards and also lasts longer. The solutions were obtained by going from N_2 (cf. fig. 9) first towards smaller and then towards larger azimuth values. The azimuth measured with respect to N_2 is denoted by ψ.

---

[12]) See the article by N. F. Verster in Sector-focused cyclotrons (Proc. Conf. Sea Island, Georgia, 2-4 February 1959), p. 199-202.

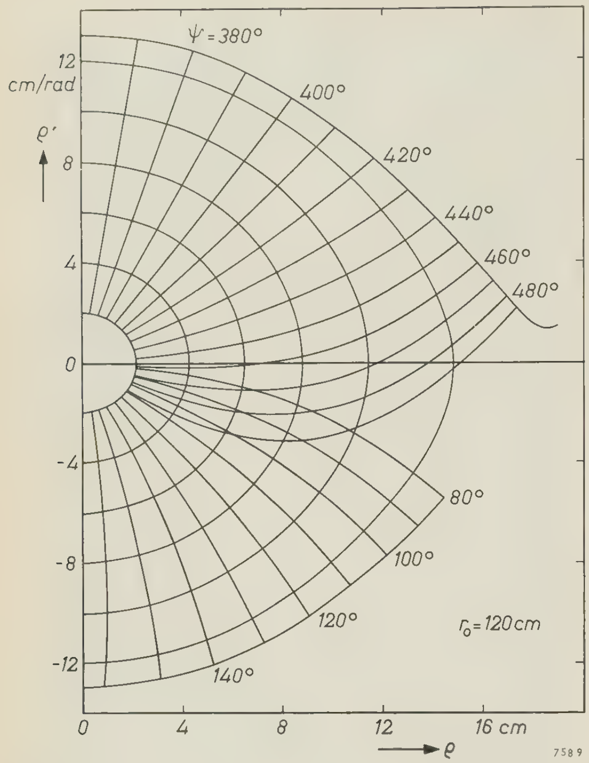

Fig. 22. Phase plot characterizing the nature of the free radial oscillation of an ion in a cyclotron. The deflection ϱ is plotted versus its derivative ϱ' ($= \mathrm{d}\varrho/\mathrm{d}\Theta$). The left half of the figure (ϱ negative) is omitted. A stable (undamped) oscillation of specific amplitude is represented by a closed curve, a harmonic oscillation by an ellipse. (In the scale on which the figure is drawn the ellipses appear as circles.) In the case of large-amplitude oscillations the influence of the boundary field is clearly visible: the curves become ovoid. The lines through the origin are lines of equal "phase" η (see fig. 9). Since the oscillation frequency is not as a rule identical with the cyclotron frequency, the isophase lines for 80° and 440°, for example, do not coincide. The figure relates to oscillations of the ions in the Orsay cyclotron about an equilibrium orbit of 120 cm radius.

Apart from in a figure of the type of fig. 9, the nature of the oscillation can also be represented graphically in a "phase plot", which shows how the deflection ϱ of an oscillation having a specific amplitude varies with the radial "velocity" ϱ'. For every stable oscillation a closed curve is produced, and for a sinusoidal oscillation an ellipse (*fig. 22*). This is a particularly clear method of presentation.

In the regenerator the ion undergoes a change in direction, but r remains unchanged (see eq. 10a) and therefore the same applies to ϱ. In the phase plot the point that descibes the situation thus drops a distance $(r/r_0)^2 I(r)$ vertically downwards at a certain moment (see eq. 10b). Generally speaking the phase η of the radial oscillation has a different value in every successive revolution. As can be seen, an oscillation of $\Theta = +0$ to $\Theta = 2\pi - 0$ (eq. 10) is entirely governed by ϱ_0' and η.

Let us now examine the vertical behaviour. We again consider one revolution from $\Theta = +0$ to $\Theta = 2\pi - 0$, of an ion whose radial oscillation is ϱ_0', η. If we describe the behaviour by means of the vector $\mathbf{z}$, whose components are z and z' — just as we described the radial oscillation by the phase plot of ϱ against ϱ' — then since the vertical orbit equation (8) is linear in z, we can find the components of $\mathbf{z}(2\pi - 0)$ from those of $\mathbf{z}(+0)$ via a set of two linear equations. Putting the four coefficients of these equations into matrix form $||P(\varrho_0',\eta)||$, we then have

$$\mathbf{z}(2\pi - 0) = ||P(\varrho_0',\eta)||\, \mathbf{z}(+0) \,. \quad . \quad . \quad (12)$$

The elements of the matrix $||P||$ — i.e. the four coefficients — can be found, by the method indicated in *fig. 23*, from the two independent solutions of eq. (8) using respectively the initial conditions $z = 0$, $z' = 1$ cm/rad and $z = 1$ cm, $z' = 0$.

We write equations (11), which describe the influence of the regenerator on z and z', likewise in matrix form:

$$||R|| = \begin{Vmatrix} 1 & 0 \\ \left(\dfrac{r}{r_0}\right)^2 \dfrac{\mathrm{d}I}{\mathrm{d}r} & 1 \end{Vmatrix},$$

and we thus have for a complete revolution:

$$\mathbf{z}(2\pi + 0) = ||R|| \times ||P||\, \mathbf{z}(+0) = ||A||\, \mathbf{z}(+0). \quad (13)$$

Eq. (6) still holds for small ϱ_0' and we have

$$||P|| = \begin{Vmatrix} \cos 2\pi\omega & \dfrac{1}{\omega} \sin 2\pi\omega \\ -\omega \sin 2\pi\omega & \cos 2\pi\omega \end{Vmatrix},$$

so that the determinant $|A|$ is equal to 1. It can be proved that this also holds for large ϱ_0' (provided we use for the orbit equation a form in which — as in (8) — there is no term with z'). If we examine a

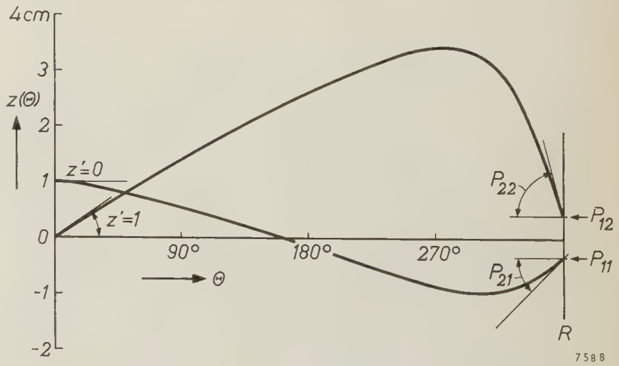

Fig. 23. The four elements of the matrix $||P(\varrho_0',\eta)||$ defining the change which the vertical oscillation state (z,z') of an ion undergoes outside the regenerator R in one revolution, are found by solving for the revolution concerned the vertical orbit equation with the initial conditions $z = 0$, $z' = 1$ and $z = 1$, $z' = 0$, also taking into account the radial oscillation. The two values of z and the appertaining slopes of the curves at the end of the revolution give the four elements in question. The curves shown here hold for the case $r_0 = 120$ cm, $\varrho_0' = 13.0$ cm/rad and $\eta = 110°$.

group of ions of identical amplitude h but different phases, we find that the points in the z,z' plane which characterize the state of oscillation of these ions together constitute an ellipse of surface area $\pi\omega h^2$. From the fact that $|A| = 1$, it may be inferred that, however the shape of this ellipse may vary from revolution to revolution, the enclosed area remains constant.

During the period of the extraction in which the amplitude is small (period c) the form of $||A||$ changes very little per revolution ("adiabatic process"). During the period d, however, there is such a marked variation in $||A||$ that it is necessary to calculate the elements of the matrix separately for each new revolution. Because the period c (small amplitude) comprises a very large number of revolutions, it is not possible for this period to follow the change of state per revolution with the matrix method. On the other hand, in period d this is the only possible method.

A practical method of mathematically treating the behaviour during period c, both for radial and vertical oscillations, has been given by Le Couteur [8]. We shall mention only the results.

In the first place it is found, as mentioned in Part II, that the phase η, which at the beginning of the deflection was still entirely governed by the free oscillation originally present, converges towards a certain fixed value. This value is determined solely by the cyclotron and regenerator field and is independent of the initial phase. In the second place this theory yields the z,z' ellipse. (We are again concerned with a group of ions of initially identical amplitude and arbitrary phase.) Thirdly, the theory indicates at what point the "deflection" begins, namely on the radius where

$$\mathrm{d}I/\mathrm{d}r = 2\pi(1-\sqrt{1-n})\sqrt{1-n}\,. \quad . \quad . \quad (14)$$

Further, with a view to vertical stability, the value of $\mathrm{d}I/\mathrm{d}r$ must lie within specific limits in the entire regenerator field.

Starting from the value of η and from the z,z' ellipse as yielded by Le Couteur's theory for a given variation of $B(r)$ and $I(r)$, the orbit described by an ion during the last period of the extraction can be found using the ϱ, ϱ' diagram (fig. 22) and the form of the matrix $||A||$ calculated per revolution.

When the extraction system was designed the variation of $B(r)$ was already established, and it was therefore necessary to look for a matching variation of $I(r)$. Since, at $r_0 = 120$ cm, the radius at which we wanted the deflection to begin, the field index n has the value 0.11, we had to ensure that $\mathrm{d}I/\mathrm{d}r$ on this radius would acquire the value 0.34; see eq. (14). Further, the given azimuthal position of the channel mouth was 60° in front of the regenerator ($\Theta = 300°$). The most suitable variation of $I(r)$ was now found by working from back to front, i.e. by beginning with the last period of the extraction.

The first step was to solve eq. (7) for various values of ϱ_0' and the chosen r_0 value of 120 cm [13]. The ϱ, ϱ' phase plot obtained in this way has already been shown in fig. 22.

Next, eq. (8) for the vertical motion was solved in the manner earlier described for each of the orbits of fig. 21 and for a number of chosen values of η between 100° and 150°. This was done in all cases over an interval from $\psi = \eta$ to $\psi = \eta + 360°$. Fig. 23 gave an example of such a solution. The matrix $||P||$ was found in all cases by interpolation from these data (see fig. 23). As regards the form of $z(\Theta)$ in this figure, it should be noted that the maximum value, measured in centimetres, is roughly 3.5 times greater than the initial slope z' measured in cm/rad. It was found that this relationship holds approximately in all instances, and we shall use this rule of thumb in our following considerations. The value of Θ at which the maximum occurs (about 270°) is also in all cases roughly the same.

To work as systematically as possible in finding a suitable $I(r)$, we looked only for functions for which the phase remained constant during the last revolutions. These can easily be derived from the phase plot (fig. 22) by inserting the isophase lines $\psi = \eta$ and $\psi = \eta + 360°$ and then measuring the vertical distance between these lines for various values of ϱ. In this way one finds the variation of $-(r/r_0)^2 I(r)$ with ϱ and hence the variation of $I(r)$. In the region of small ϱ values the curves were extrapolated so as to make them tangent to the line $I = 0.34\,\varrho$ at the origin (see above). The result is presented in *fig. 24*. It was found that the curves can be represented to a good approximation by the formula $I = 0.34\varrho + \beta\varrho^2$.

In order to construct the ion orbits in period d for each of the regenerator functions thus found, we first computed the z, z' ellipse at the end of the penultimate extraction period, and also the (radial) phase η. As we have seen, the latter converges to a constant value, i.e. to the value at which it remains fixed in the last extraction period. (It should be noted here that it is not so important to know η for describing the penultimate extraction period itself; it is only in the period where the amplitude is large that we need to know η.) With the aid of these data we then

---

[13] The calculations were carried out using the small experimental computer PETER, made in the Philips Research Laboratories and which was available at the time.

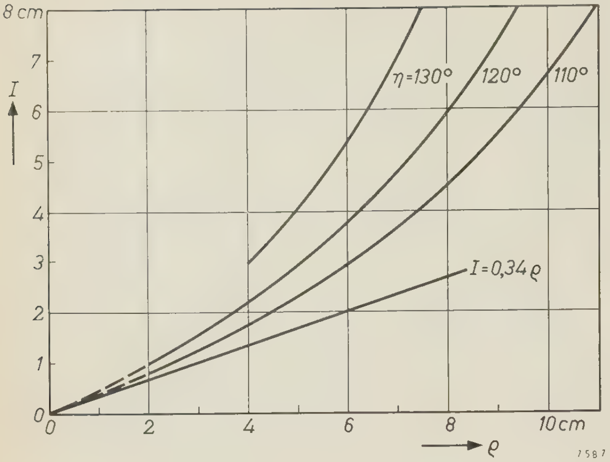

Fig. 24. The required form of the regenerator field I as a function of r, for regenerators that keep the phase η of the oscillations constant. The curves are derived from the phase plot in fig. 22. The quantity ϱ ($= r - r_0$) is plotted as abscissa. The curves hold for the indicated values of η. In the origin they are all tangent to the straight line $I = 0.34\ \varrho$.

constructed the further course of the orbits for various initial conditions: the radial oscillation from the phase plot and the two isophase lines referred to, and the vertical oscillation from the matrix $||A||$, the elements of which can be calculated (eq. 13) now that $||P||$ and $I(r)$ are known. As mentioned, the latter calculation had to be repeated for every revolution.

The radial distance between the ultimate and penultimate revolutions of the ions arriving in the channel mouth, and also the position of the (virtual) source of the ion beam entering the channel, can directly be found from these calculated orbits. (The positions of the virtual source derived from the vertical divergence will not necessarily coincide with that found from the horizontal.)

Now it was found that, to obtain a suitable radial increase of ϱ combined with a not unduly large vertical amplitude, the value of η had to be chosen between 110° and 130°. This may be inferred from *fig. 25.*

This figure shows the upper and lower limits of $\mathrm{d}I/\mathrm{d}r$ which must not be exceeded if vertical "stability" is to be ensured, plotted against ϱ for

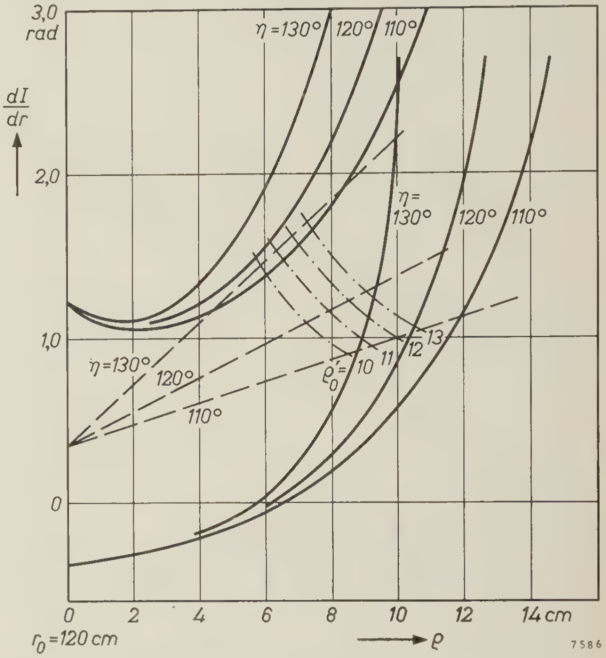

Fig. 25. Characteristics of regenerators with constant phase, as required to ensure stability of the ion orbits against vertical oscillations. The radial gradient $\mathrm{d}I/\mathrm{d}r$ of the regenerator field is plotted versus the radial coordinate ϱ. The solid curves represent the stability limits; each pair of curves relate to the indicated value of the phase angle η. The dashed lines represent the variation of $\mathrm{d}I/\mathrm{d}r$ for regenerator fields with constant phase (value also indicated). The dot-dash lines represent the loci of points having the same value of ϱ_0'; the indicated values are in cm/rad.

Table III. Principal data of the three carefully analysed regenerator fields ($r_0 = 120$ cm). The figures relate to the orbits of ions which, in their last revolution, pass the equilibrium orbit with a slope of 13 cm/rad.

Regenerator field	Characteristic quantities of ion revolution			In the regenerator ($\Theta = 360°$)			At the channel mouth ($\Theta = 300°$)		Line 1 to 4: the matrix $\|\|A\|\|$ Line 5: $\|\|P(\Theta = 300°)\|\|$				$z_{\max}/h$ for three azimuth values		
	No.	ϱ_0'	η	ϱ	I	$\left(\frac{r}{r_0}\right)^2 \frac{\mathrm{d}I}{\mathrm{d}r}$	ϱ	ϱ'	A_{11}	A_{12}	A_{21}	A_{22}	$\Theta = 0°$	$\Theta = 270°$	$\Theta = 300°$
I_1	$n-4$	3.4	121°	3.4	1.72	0.68			−0.38	2.78	−0.49	0.96	0.98	1.5	
	$n-3$	4.6	121°	4.5	2.54	0.82			−0.38	2.65	−0.52	0.99	0.98	1.5	
	$n-2$	6.1	121°	6.2	4.01	1.01	5.5	3.3	−0.39	2.33	−0.54	0.65	0.93	1.5	
	$n-1$	8.5	121°	9.1	7.28	1.35	7.6	4.9	−0.38	1.36	−0.39	−1.25	0.88	1.5	
	n	**13.0**	120°				11.7	8.1	−0.48	3.27	−0.11	−1.37	0.52	2.6	2.6
I_2	$n-4$	3.0	124°	2.8	1.50	0.75			−0.37	2.77	−0.52	1.20	1.00	1.5	
	$n-3$	4.0	124°	3.8	2.32	0.90			−0.36	2.67	−0.55	1.33	1.00	1.5	
	$n-2$	5.4	124°	5.3	3.79	1.12	5.1	2.7	−0.36	2.42	−0.60	1.25	1.00	1.6	
	$n-1$	7.8	125°	8.1	7.38	1.52	7.3	4.1	−0.35	1.73	−0.63	0.23	0.95	1.6	
	n	**13.0**	125.5°				12.3	7.5	−0.28	3.16	−0.16	−1.74	0.62	1.8	1.7
I_3	$n-4$	2.5	130°	2.1	1.16	0.77			−0.36	2.78	−0.54	1.36	1.02	1.6	
	$n-3$	3.3	130°	3.0	1.95	0.97			−0.34	2.68	−0.58	1.63	1.02	1.6	
	$n-2$	4.8	129°	4.5	3.87	1.27	4.6	2.0	−0.33	2.50	−0.66	1.88	1.07	1.7	
	$n-1$	7.3	130°	7.2	7.64	1.88	7.1	3.2	−0.32	1.76	−0.77	1.09	1.13	2.0	
	n	**13.0**	130.2°				13.0	6.9	−0.16	3.02	−0.22	−2.09	0.73	1.6	1.4

three values of η, and also the variation of $\mathrm{d}I/\mathrm{d}r$ with ϱ for the regenerator fields corresponding to these η values (dashed lines of slope 2β). The dot-dash lines in this figure are curves of constant ϱ_0'. From the latter one can find the maximum value of ϱ_0', i.e. the maximum useful amplitude corresponding to the relevant value of η. As can be seen, this increases with η.

It is not in the least necessary, however, to try to make ϱ'_0 as large as possible. At the position of the channel mouth ($\Theta = 300°$) the value of $\varrho_n - \varrho_{n-1}$ (which increases with ϱ_0' and η) need not be made larger than is necessary for "peeling off" the ions (e.g. 5 cm). By making the value larger we only reduce the fraction of the ions entering the channel mouth. A reasonable compromise is obtained with a value of about 120° for η.

On the basis of these results we made a closer analysis of three regenerator fields, having the β values 0.05, 0.07 and 0.09. We call these fields respectively I_1, I_2 and I_3. The value of η for these fields is not exactly constant — the formula $I = 0.34\varrho + \beta\varrho^2$ was no more than a good approximation — and it therefore had to be determined for each revolution. As initial values we chose those underlying the construction of the curves in fig. 24. The values for revolutions with greater amplitudes were found by drawing the relevant orbit in the ϱ, ϱ' plane. From a point having the initial η value we draw a line on the ϱ,ϱ' curve to the point with phase $\eta + 360°$, and then go vertically downwards over the distance corresponding to $I(r)$. In this way we reach the isophase line corresponding to the new phase, and so on. In addition we constructed for all three fields the orbit ending with an oscillation for which $\varrho_0' = 13$ cm/rad. From this the components of $||P||$ were computed in the manner described, and then those of $||A||$, using $I(r)$. The results are collected in *Table III*. It can be seen that the elements of $||A||$ only begin to change markedly during the last two revolutions. Up to the orbit $n - 2$ we therefore used the z,z' ellipse applicable, according to Le Couteur's theory, to the first period. (It will be recalled that this ellipse describes the state of oscillation of a group of ions of initially identical amplitude and arbitrary phase after leaving the regenerator ($\Theta = +0$).) This then, gives the vertical structure of the ion beam at the beginning of revolution $n - 1$. From this point onwards the structure was calculated using the relevant form of the matrices $||P||$ and $||R||$. The result is shown in *fig. 26*. The five ellipses, drawn in each figure, apply respectively to the end of revolution ($n - 2$), i.e. just in front of the regenerator, to the beginning of revolution ($n - 1$), i.e. just behind the regenerator, and so on. The last one applies at the location of the channel mouth. In fig. 26 ellipse *2* is thus the one which was computed by Le Couteur's

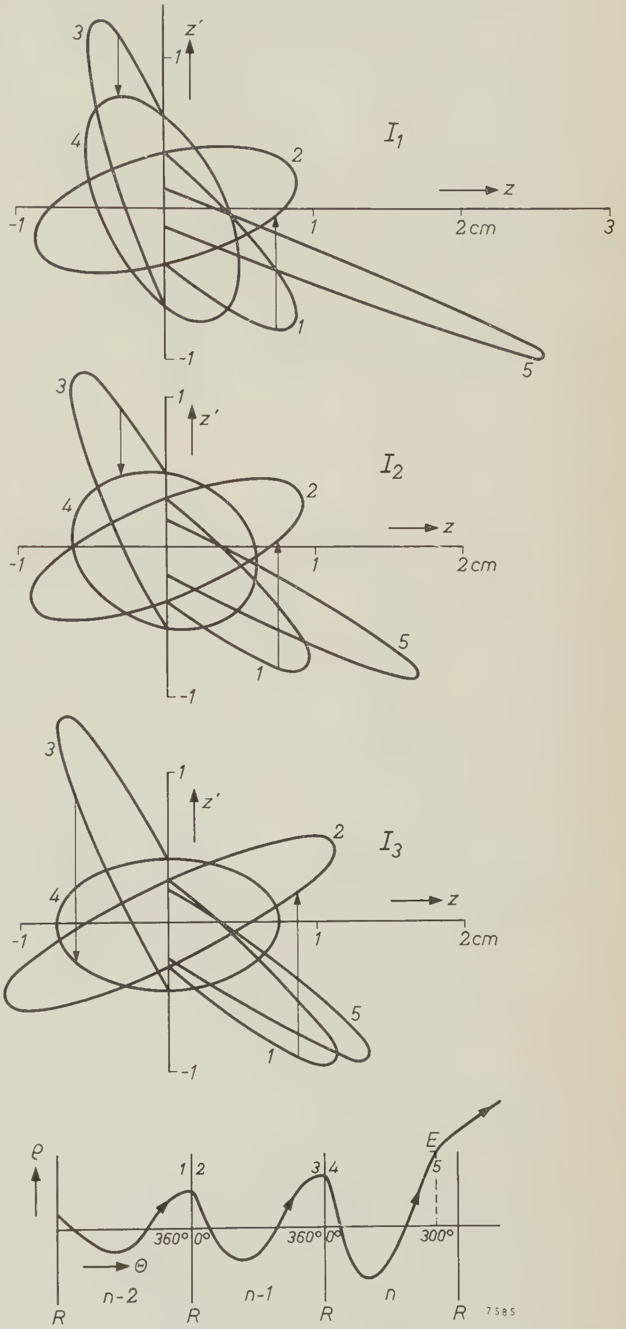

Fig. 26. The vertical structure of the ion beam during the last two revolutions, for the three completely calculated regenerator fields I_1, I_2 and I_3, and relating to a group of ions which, before the beginning of the extraction process, had the same vertical amplitude and arbitrary phase. This structure is described by an ellipse in the z,z' plane, which gradually changes its shape and position with increasing ϱ, but not its surface area. For clarity, only the halves of some ellipses are shown. Ellipses *1* to *5* relate to the following points (see bottom waveform and also fig. 9): *1* at the end of revolution ($n - 2$), just before the regenerator; *2* at the beginning of revolution ($n - 1$), just behind the regenerator; *3* at the end of revolution ($n - 1$); *4* at the beginning of revolution n; *5* at the channel mouth. The vertical arrows represent the change in z' produced in an arbitrary ion when it passes the regenerator. The arrow between the ellipses *1* and *2* and that between *3* and *4* in each diagram do not refer to the same ion.

method. Ellipse *1* was found by working backwards.

Since, as we have seen, the maximum deflection in the z direction is roughly $3.5z'_{\max}$ $(+0)$ in the last revolution (see fig. 23), we must ensure that ellipse *4* in fig. 26 is not too high. From this standpoint, the regenerator fields I_2 and I_3 are preferable to I_1. From these two we made our final choice of I_2, because the relevant regenerator is somewhat easier to realize, and also because the difference $\varrho_n - \varrho_{n-1}$ at $\Theta = 300°$ was 5 cm in this case, which is sufficient, as against 6 cm in the case of field I_3. *Fig. 27* gives a representation in the ϱ,ϱ' plane of the orbit of an ion which, under the influence of the regenerator, finally arrives in the channel. For constructing the orbit curve in this figure, use was made of the $I(r)$ function of the actual regenerator; this I function is practically identical with I_2.

Summarizing the principal characteristics of the regenerator, and of the method of treatment described in Part III of this article, we note first of all that we have obtained a regenerator which, at the end of the last extraction period, causes a sufficiently large increase in the radial coordinate of the ions per revolution at $\Theta = 300°$ without substantially increasing the height of the beam. The method of computation outlined also makes it possible to investigate quickly, during the construction of an extraction system, the influence of discrepancies between the regenerator field chosen on theoretical grounds and that which is present at a given moment. It takes a great deal of time to obtain a desired field exactly, and it is therefore of great importance to be able to investigate what deviations are tolerable. Fortunately, these were found to be fairly considerable in the region of the last revolution. Turning again, for instance, to the z,z' ellipses for I_2 (fig. 26), we see that the arrow which describes events during the last passage of the regenerator can comfortably be about 20% shorter or about 40% longer: the shape of ellipse *4* — which cuts ellipse *3* on the z' axis — is not changed thereby sufficiently to seriously affect the maximum value of z', which of course determines the maximum value of z. Since the length of this arrow is proportional to the gradient $\mathrm{d}I/\mathrm{d}r$ of the regenerator field (see eq. 11b), the tolerable variation mentioned also applies to the latter quantity.

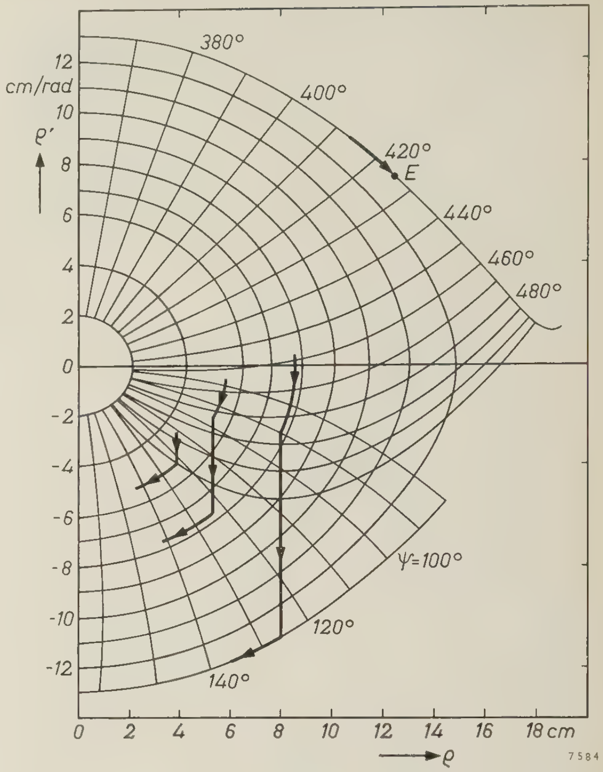

Fig. 27. Phase plot of the Orsay cyclotron (cf. fig. 2) showing the last three revolutions of an ion which finally arrives in the channel. The point E represents the state upon entering the channel.

The effect of a change in I for large ϱ on the radial behaviour can be seen from fig. 27. In this figure the above variation of I results in a proportional variation of the largest of the vertical lines. As regards the orbit drawn in the figure, this means that the bottom of the line comes to lie somewhat higher or lower. The phase η for large ϱ does not therefore remain constant but either increases or decreases slightly. If we construct for the new phase line the orbit that ends at E, we find that, as far as the increase of ϱ during the last revolutions is concerned, this orbit is hardly less suitable than the drawn one.

Summary. The synchrocyclotron built by Philips at Orsay for the University of Paris is capable of accelerating protons up to about 160 MeV, and deuterons up to about 80 MeV. The RF system, with flywheel circuit, is designed to enable a change-over to be made from proton to deuteron frequencies by means of a simple structural alteration. A radially adjustable target makes it possible to produce a neutron beam of variable energy. By means of a beam-extraction system an external beam (proton energy 157 MeV) is obtained whose intensity, depending on the current, is 5 to 12% of that of the internal beam. The extraction system induces a radial oscillation of the ions around their equilibrium orbit, enabling the ions to enter a magnetic channel without being lost by collision with the channel wall, and without the radius having to be so large as to make the equilibrium orbit coincide with the circle on which the field index has the dangerous value of 0.2. The ions are then extracted through the magnetic channel. The oscillations begin when the orbit radius is 120 cm and are generated by a local field disturbance having a positive radial gradient, produced by a device referred to as a regenerator. The amplitude of the vertical oscillations remains small because the ions in part of their orbit enter the fringing field (where the gradient is strongly negative). A detailed treatment is given of the calculations used to find a suitable form of regenerator. Also discussed are the construction of regenerator and channel, an investigation of the magnetic field using a copper wire to simulate the ion orbits and further the adjustment of regenerator and channel, likewise using the orbit simulator.

ABSTRACTS OF RECENT SCIENTIFIC PUBLICATIONS BY THE STAFF OF N.V. PHILIPS' GLOEILAMPENFABRIEKEN

Reprints of those papers not marked with an asterisk * can be obtained free of charge upon application to Philips Electrical Ltd., Century House, Shaftesbury Avenue, London W.C. 2, where a limited number of reprints are available for distribution.

2932: B. G. van den Bos: Investigations on pesticidal phosphorus compounds, III. The structure of the reaction product of 3-amino-5-phenyl-1,2,4-triazole and bis(dimethylamido)phosphoryl chloride (WP 155) (Rec. Trav. chim. Pays-Bas **79**, 1129-1136, 1960, No. 11).

The reaction of 3-amino-5-phenyl-1,2,4-triazole with *bis*(dimethylamido)phosphoryl chloride gives a compound (WP 155) with a strong anti-mildew effect. Comparison of the UV absorption spectra of a bromine compound derived from WP 155 and the three N-ethyl-3-bromo-5-phenyl-1,2,4-triazoles with those of the three known N-methyl-3-methyl-5-phenyl-1,2,4-triazoles indicates that WP 155 is 5-amino-1-[*bis*(dimethylamido)phosphoryl]-3-phenyl-1,2,4-triazole.

2933: J. H. Uhlenbroek and J. D. Bijloo: Investigations on nematicides, III. Polythienyls and related compounds (Rec. Trav. chim. Pays-Bas **79**, 1181-1196, 1960, No. 11).

Part of an investigation of the possibilities of using polythienyls as nematicides (i.e. for control of eel-worms; see also these abstracts, Nos **2692**, **2743** and **2786**). A number of isomeric polythienyls and some mixed polyphenylthienyls were tested as to their nematicidal effect. All compounds which gave good results proved to be derivatives of 2,2′-bithienyl. Some new compounds are described, e.g. 2,3′-4′,2″-terthienyl, 1,4-di(2-thienyl)-benzene and various methyl polythienyls.

2934: J. R. Roborgh and Th. J. de Man: The hypercalcemic activity of dihydrotachysterol$_2$ and dihydrotachysterol$_3$ and of the vitamins D$_2$ and D$_3$ after intravenous injection of the aqueous preparations, II. Comparative experiments on rats (Biochem. Pharmacol. **3**, 277-282, 1960, No. 6).

Vitamin D$_2$, vitamin D$_3$ and the dihydrotachysterols derived from them have a hypercalcemic effect (i.e. they can increase the calcium content of the blood serum). In an earlier investigation (these abstracts No. **2785**) it was shown that, when orally administered as a solution in oil, dihydrotachysterol$_3$ had the greatest effect, followed by dihydrotachysterol$_2$, vitamin D$_3$ and vitamin D$_2$. The same order of activity is found when these compounds are injected intravenously as an aqueous dispersion. The blood serum shows the highest calcium content two to four days after administration. The relative activities of the various compounds are found to depend strongly on the length of time which elapses between the administration of the preparations and the sampling of the blood sera, and are in reasonably good agreement with the results of the previous investigation.

2935: W. Duyfjes: Interfacial phenomena in pesticide application (Pest Technol. **2**, 239-243, 1960, No. 11).

Many pesticides are applied in aqueous media. Since most of them are not soluble in water, they must be used as an emulsion or suspension. A number of physical problems which arise in this connection in the formulation of pesticides are discussed in this publication. See also Philips tech. Rev. **19**, 165, 1957/58.

2936: E. W. Gorter: Some structural relationships of ternary transition metal oxides (XVIIth International Congress of Pure and Applied Chemistry, Munich 1959, Part I, pp. 303-328, Verlag Chemie, Weinheim 1960).

The oxides of metals of the first transition group have been much studied, because they can be put to many uses. This article deals only with compounds of the type B_nO_p and $A_mB_nO_p$, where B is a cation which can fit in the interstices of a close-packed array of oxygen ions, e.g. a transition-metal ion, and A is a cation which is too large for this. A new method of describing crystal structures is discussed, where the crystal is imagined to be cut up into a number of blocks by planes mid-way between crystallographically equivalent or chemically identical atoms. This method is illustrated by listing all the ways in which an ion of a close-packed array can be surrounded by six-coordinated cations, and discussing all the structures thus obtained.

The different ways of modifying simple oxides by substitution and the formation of superstructures are discussed for the cases of the NaCl, spinel, corundum and rutile structures. A number of existing compounds of the type $A_mB_nO_p$ are shown in an A-B-O diagram. The structural relationships between a number of compounds near the point ABO_3, and between others near the points B_2O_3 and B_3O_4, are discussed.

2937: J. H. Spaa: A rapid indicating instrument for the stepwise measurement of airdust radioactivity (Progr. nucl. Energy, series 12 (Health Physics) **4**, 25-31, 1960).

Description of an instrument for the rapid detection of radioactive dust in the air, which has already been described in abstract No. **2823a.** The present article also discusses the experience gained with the instrument.

2938: F. K. Lotgering: Topotactical reactions with ferrimagnetic oxides having hexagonal crystal structures, II (J. inorg. nucl. Chem. **16**, 100-108, 1960, No. 1/2).

If a mixture of powdered oxides of the system BaO-MeO-Fe_2O_3 (where Me = Co, Ni, Zn, etc.) consists *in part* of an oxide which can be magnetically oriented, while the rest of the sample cannot, then if the mixture is heated after magnetic orientation, the reaction product is often found to consist of a single-phase oxide which is *highly* oriented. Such reactions have been given the name "topotactical reactions" (see these abstracts No. **2707**). The present publication deals with an investigation of the mechanism of various topotactical reactions, and of the effect of sintering on the degree of orientation of the reaction products. See also Philips tech. Rev. **20**, 354, 1958/59.

2939: J. N. Walop, Th. A. C. Boschman and J. Jacobs: Affinity of N-acetylneuraminic acid for influenza virus neuraminidase (Biochim. biophys. Acta **44**, 185-186, 1960, No. 1).

Preliminary report of a new method for the determination of neuraminidase activity. The system of influenza virus and N-acetylneuraminyllactose is found to follow Michaelis-Menten kinetics. It is shown that N-acetylneuraminic acid (NANA) is a competitive inhibitor of this reaction. Comparison of the inhibitor constant with the Michaelis constant for the substrate shows that the affinity of NANA for the enzyme molecule is strengthened 8-fold by the ketosidic linkage of the NANA moiety to lactose.

2940: W. Albers and J. Th. G. Overbeek: Stability of emulsions of water in oil, III. Flocculation and redispersion of water droplets covered by amphipolar monolayers (J. Colloid Sci. **15**, 489-502, 1960, No. 6).

It is shown by simple calculations that emulsions of water in oil cannot be sufficiently protected against flocculation by an adsorbed layer of amphipolar molecules with an oleophilic chain of about 20 Å at the surface of the water droplets. Neither does the combination of electrical charge and adsorbed layer prevent flocculation. It might however be expected that the flocculated system could be redispersed by means of not too large shearing forces. This is confirmed by viscosity measurements. Non-Newtonian behaviour found at low rates of shear is a consequence of flocculation. From the minimum rate of shear required to reach the Newtonian region (where the rate of shear is a linear function of the shear stress), i.e. to cause complete redispersion, the effective Van der Waals constant A between the water droplets can be estimated. The value of $A = 4 \times 10^{-15}$ erg is found.

2941: J. L. Meijering: Hardening by internal oxidation as a function of velocity of the oxidation boundary (Trans. Metall. Soc. AIME **218**, 968-971, 1960, No. 6).

The hardness of small metal cylinders or spheres which have been hardened by internal oxidation first decreases with increasing distance from the surface, but then increases again. This is in agreement with the theory that the change in hardness is mainly determined by the change in the rate of advance of the oxidation boundary, which velocity determines the dispersion of the oxide.

2942: H. J. L. Trap and J. M. Stevels: Conventional and invert glasses containing titania, Part 2 (Phys. Chem. Glasses **1**, 181-188, 1960, No. 6).

Investigation of the variation in the dielectric properties of silicate glasses containing PbO as the various components are gradually replaced by TiO_2. The observed effects can be satisfactorily explained on the basis of considerations on the behaviour of titanium ions in glass given in a previous publication (these abstracts, No. **2906**). The addition of the titanium ion usually improves the dielectric properties. The infrared spectra of the investigated glasses are also in agreement with the above-mentioned considerations. See also Philips tech. Rev. **22**, 300, 1960/61 (No. 9/10).

2943: E. Havinga, R. J. de Kock and M. P. Rappoldt: The photochemical interconversions of provitamin D, lumisterol, previtamin D and tachysterol (Tetrahedron **11**, 276-284, 1960, No. 4).

A summary of the results of recent investigations into the photochemical isomerizations in the vitamin D field which have been the subject of research during the last decade. A new scheme is proposed showing the various reactions occurring during irradiation of a provitamin D. The quantum yields of these reactions at 2537 Å were determined. On the basis of these data the effect of the wavelength of the light used on the yields of products is explained. Emission spectra of ergosterol and its photoisomers were measured at 80 °K. No phosphorescence was observed. Some aspects of the mechanism of the photochemical cyclizations, ring openings and the cis/trans isomerization are discussed.

2944: G. Hardeman: La polarisation dynamique nucléaire dans du polytétrafluoréthylène irradié (Bull. Group. Inf. mut. AMPERE **9**, No. spéc. (compte rendu 9e Coll., Pisa, 12-16 Sept. 1960), 669-673, 1960). (Nuclear dynamic polarization in irradiated polytetrafluorethylene; in French.)

See these abstracts No. **R 410.**

2945: S. van Houten: Semiconduction in $Li_xNi_{(1-x)}O$ (Phys. Chem. Solids **17**, 7-17, 1960, No. 1/2).

NiO is an insulator, which may be made conducting by the addition of lithium oxide. This behaviour can be explained in terms of an energy-level scheme consisting of full, localized Ni^{2+} levels with empty Ni^+ levels approximately 5 eV above them. The consequence of introducing lithium into the lattice is that the Li^+ ions are compensated by Ni^{3+} ions, giving ($Li^+.Ni^{2+}$) acceptor levels at approximately 0.03 eV above the Ni^{2+} levels. Electrical conduction, which is always *p*-type, may be described in terms of a thermally activated diffusion of holes from one nickel ion to another. The activation energy is connected with self-trapping by the polarization induced by the hopping hole itself. A detailed account is given of the calculation of the energy levels, starting from the ionization energies of the free ions and combining them with Madelung potentials. Corrections are made for the polarization of the lattice and for differences in crystal field stabilization between the Ni ions of different valencies. Measurements of Seebeck effect and electrical resistance as a function of temperature and lithium concentration are discussed in terms of this model. It is shown that the oxygen band, lying much lower than the Ni^{2+} levels, does not give any contribution to the electrical conduction.

2946: H. Koelmans: Association and dissociation of centres in luminescent ZnS-In (Phys. Chem. Solids **17**, 69-79, 1960, No. 1/2).

ZnS-In phosphors, which are efficient upon excitation with $\lambda = 3650$ Å, were prepared by firing in H_2S at 1200 °C and quick cooling to room temperature. The emission spectrum depends on the In concentration and consists of three bands at 6200 Å, 5350 Å and 4700 Å. X-ray analysis shows that the maximum amount of In incorporated is about 10^{-2} gram-atoms In per mole ZnS. Refiring the phosphors at 600 °C kills the luminescence at room temperature, an effect shown to be due to association; the associated centres act as killer centres. The low-temperature phosphorescence of the ZnS-In phosphors is strongly stimulated by irradiation into bands at $\lambda = 1.8\ \mu$ and $\lambda < 1.2\ \mu$.

2947: W. Nijenhuis: Benaderingsmethode van overdrachtsfuncties, waarbij een rimpel zowel in het doorlaatgebied als in het dempingsgebied wordt voorgeschreven (T. Ned. Radiogenootschap **25**, 297-306, 1960, No. 5/6). (Method of approximating frequency-response curves in which limits are set on the ripple in the pass-band as well as in the damping region; in Dutch.)

For telephony and other purposes, filters are needed with response curves in which the ripple in the pass-band and in the damping region, and the width of the transition region, are kept within (narrow) specified limits. As is known, the frequency-response curve of a filter composed of resistances, self-inductances and capacitances can always be expressed as the ratio of two rational functions. This publication describes a method, originally developed by Klinkhamer, for finding a function of this type which fulfils the above-mentioned conditions. Use is made of conformal mapping of the complex frequency plane by means of elliptical functions. The problem can be visualized by consideration of a membrane model of the response function.

2948: M. J. Koopmans: Systemic fungicidal action of some 5-amino,1-bis(dimethylamido)phosphoryl triazoles 1,2,4 (Meded. Landbouwhogesch. Opzoekingsstat. Gent **25,** 1221-1226, 1960, No. 3/4).

A discussion of the fungicidal action of the 3-pentyl and 3-phenyl derivatives of 5-amino,1-*bis*-(dimethylamido)phosphoryl 1,2,4-triazole. (The 3-phenyl derivative is on the market under the name "Wepsyn".) This group of compounds is very effective against the powdery mildew species which occur on plants such as apple trees, roses, and barley. With apple trees and barley, this effect is found on spraying of the leaves. The effect is comparable with that of 2,4-dinitro-6-capryl-phenyl crotonate ("Dinocap"). These compounds also protect the above-mentioned plants when administered to the roots. Their *in vitro* activity is much less than that of "Dinocap"; the resistance is thus apparently induced in the host plant, the effect being produced either via the leaves or via the roots.

2949: W. J. Oosterkamp and C. Albrecht: Methods of evaluating the new instrumental systems for diagnostic radiology (IXth Int. Congress of Radiology, Munich, 23-30 July 1959, Ed. B. Rajewsky, pp. 1451-1460, Thieme, Stuttgart 1960).

A short description of various new instrumental aids to X-ray diagnosis (image intensification, X-ray television and various combinations of these) is followed by a discussion of the effect of radiation contrast, noise and blurring on the perception of small details in the final picture.

2950: O. Reifenschweiler: Neutrons from small tubes, I. Philips tube: continuous or pulsed operation (Nucleonics **18,** No. 12, 69-71, 1960).

Description of a sealed neutron-generator tube, developed over the past years to meet the growing needs of neutron physics in science and engineering. The tube uses the D-T reaction to produce 3×10^8 n/sec during continuous operation. When adapted for pulsed operation, it yields a peak output of 3×10^{10} n/sec. The tube contains a Penning ion source, a 100-200-kV accelerating system, a replenisher that keeps the pressure within the tube constant, and a titanium-tritium target that is self-replenishing and, therefore, does not limit the lifetime of the tube. See also Philips tech. Rev. **23,** 325, 1961/62 (No. 11).

2951: F. L. H. M. Stumpers: Balth. van der Pol's work on nonlinear circuits (IRE Trans. on circuit theory **CT-7,** 366-367, 1960, No. 4).

A survey of the pioneering work of Van der Pol in the field of nonlinear networks (Van der Pol's equation, relaxation oscillations, etc.) in the special number on this subject which he was to edit, and which is now dedicated to his memory. (For a more complete survey of the work of Van der Pol see Philips tech. Rev. **22,** 36, 1960/61, No. 2.)

2952: W. van Gool and J. G. van Santen: Sintered cadmium sulphide, a photoconductive ceramic (Special ceramics, Proc. Symp. Brit. Ceramic Res. Ass., Ed. P. Popper, pp. 252-264, Heywood, London 1960).

A description of the preparation of photoconductive cadmium-sulphide powders and the making of compressed and sintered discs from these powders. The mechanism of photoconduction is discussed and it is shown that measurement of the properties of photoconductive ceramics could give additional information about the sintering process. The controlled preparation following the methods described makes possible a reproducible large-scale production of highly sensitive photoresistors. See also Philips tech. Rev. **20,** 277, 1958/59.

2953: M. P. Rappoldt and P. Westerhof: Investigations on sterols, XIX. 6-dehydro-9β,10α-progesterone from pregnenolone (Rec. Trav. chim. Pays-Bas **80,** 43-46, 1961, No. 1).

6-dehydro-9β,10α-progesterone is a very effective oral progestative. It was originally made from lumisterol$_2$. It is however also possible to start from pregnenolone (pregn-4-en-3β-ol-20-one), which is more readily available. Bromination of this compound followed by dehydrobromination gives pregna-5,7-dien-3β-ol-20-one, which yields the 9β,10α isomer when irradiated with ultraviolet light. Oppenauer oxidation followed by isomerization by means of HCl in isopropanol gives the desired end product.

Now available

H. Zijl: Large size perfect diffusors (Philips Technical Library, 1960, 196 pp., 120 figures, 49 graphs).

Second edition (with minor alterations) of the book which has already been reviewed in Philips tech. Rev. **15,** 262, 1953/54.

THE UNIVERSITY OF ILLINOIS AT CHICAGO
3 8198 316 049 723